Weierstrass Representations of Minimal Surfaces
and
the Costa Surface

Daniel Young

February 11, 2022

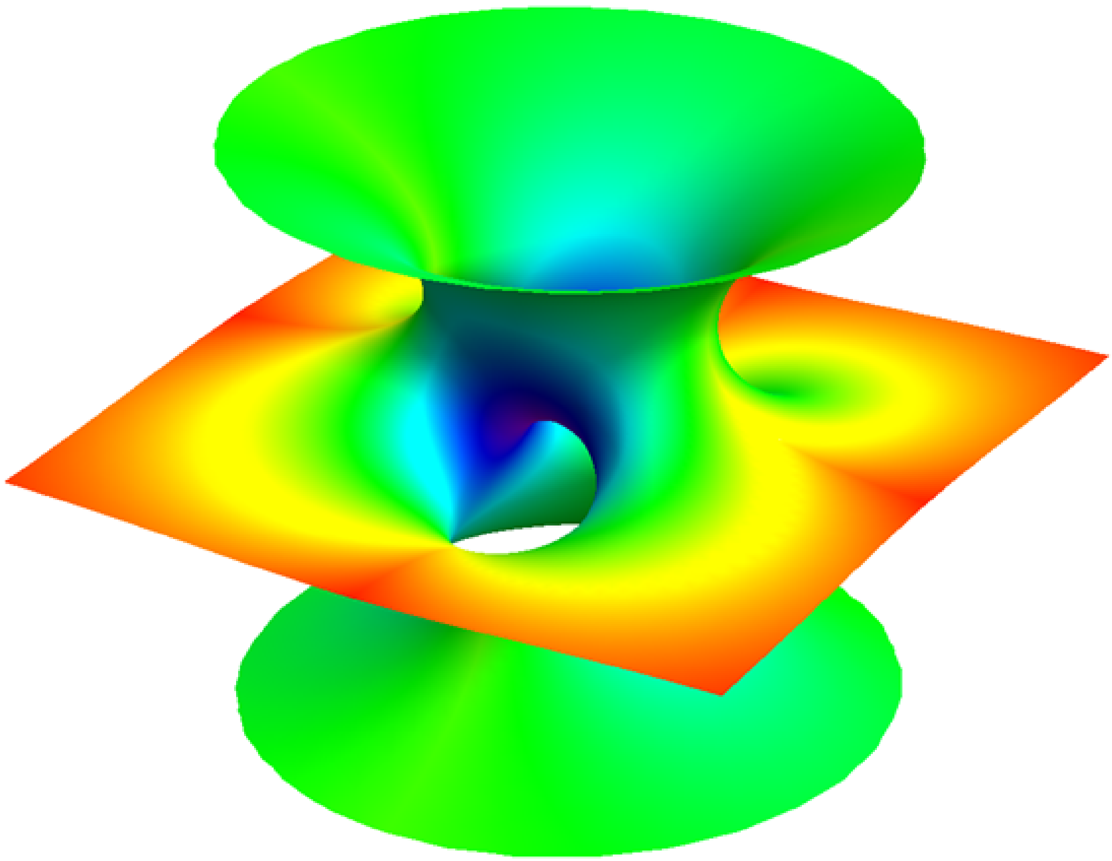

Figure 1: A plot of the Costa surface near the origin.

Abstract

In this paper we shall rigorously define minimal surfaces and some theorems relating to them. We shall then use complex analysis to derive the Weierstrass representation. We shall start with a basic definition of minimal surfaces and show that this gives rise to a rich structure which can be studied.

Then we will study the properties of some canonical examples of minimal surfaces and graph them. We shall calculate the exact equation for Enneper surface, the catenoid and the helicoid. We also prove that the catenoid and helicoid have a deep relationship, naturally arising from a whole family of minimal surfaces.

Finally we will explore the Weierstrass representation of the Costa surface and its symmetries in detail, focusing on how these arise from the symmetries of its Weierstrass representation. Finally we shall also explore the associate family of the Costa surface, something which is rarely, if ever discussed in the literature.

Contents

1 Introduction

Minimal surfaces are surfaces which locally minimise surface area [1]. The study of minimal surfaces was born when Joseph Lagrange successfully used calculus of variations to work out the differential equations that minimise the area of a surface. Over the next few years, the first examples of minimal surfaces began to appear, but progress in the field was slow. Karl Weierstrass and Alfred Enneper made a huge breakthrough in the subject by unifying the study of minimal surfaces with complex analysis. They did this through deriving what is known as the Weierstrass representation, which we will study in this paper. With this powerful tool, infinitely many minimal surfaces could be generated and studied. We will set up and explore Weierstrass representation, and see how it can give insight into the properties of minimal surfaces.

Another key mathematician in the study of minimal surfaces was Jean Meusnier. He discovered the helicoid and the catenoid as well as some other important properties we will use in this paper. (He is also sometimes credited as the inventor of dirigible airships [2]!)

A great example of a minimal surface is soap films: if a closed wire loop of any shape is dipped in soapy water, the film formed when it is removed will be a minimal surface. This is because the soap film tries to minimise energy by assuming the smallest shape possible. Importantly, spherical soap bubbles are not minimal surfaces as they have no boundary. In fact any bubble that encloses a volume of air such that the air cannot escape is not a minimal surface as there is an extra constraint on the system.

Alongside soap films, minimal surfaces have a huge range of theoretical and practical applications. The study and understanding of minimal surfaces is crucial to architecture [3]: the minimising property of minimal surfaces is used to designing buildings that minimise weight and material usage.

Recent work in minimal surfaces that are triply periodic has direct applications to material science in the creation of strong, lightweight foam like materials. Here, minimal surfaces can fill space while using the least amount of material possible. These new materials are used in a variety of high performance industries, including aeronautics and space exploration.

Higher dimensional minimal surfaces also arise in the study of gauge theory [4] as well as string theory where the world sheets traced by strings are minimal surfaces. This is an interesting area of study as it could show that minimal surfaces have a direct role in shaping the fundamental physics that governs our universe.

In 1982, Brazilian mathematician Celso Costa wrote his PhD thesis [5] on what would come to be known as the Costa surface, which is a complete embedded minimal surface.

2 Mathematical Formalism of Minimal Surfaces

Informally, we can think of minimal surfaces as minimising area at each point of the surface. By this we mean given a point on a minimal surface if we restrict our surface to a small open neighbourhood around this point, and consider its boundary, then any small deformation of this restricted region keeping the boundary invariant results in an increase of surface area.

In this section we shall define the notations of a surface and various other tools and properties required to study minimal surfaces, resulting in a rigorous definition of a minimal surface.

2.1 Geometry of Surfaces Formalism

To begin with we shall by recalling some definitions from the geometry of surfaces which will give us the tools needed to describe surfaces and study their properties.

Firstly we shall mathematically describe the exact form of a surface.

Definition 1 (Surface)**.** A *surface* is a mapping from an open subset of the Euclidean plane, i.e. $D \subset \mathbb{R}^2$, into a subset of Euclidean space, $\mathbb{R}^3$. We shall use $\vec{\sigma}(u_1, u_2)$ as our surface map where $\vec{\sigma} : D \to \mathbb{R}^3$. That is to say $\vec{\sigma}$ is a function which maps the point $(u_1, u_2) \in \mathbb{R}^2$ to $\vec{\sigma}(u_1, u_2) \in \mathbb{R}^3$.

We can view $\vec{\sigma}$ as a vector of 3 functions each of which are well defined on the domain $D \subset \mathbb{R}^2$, and output values in $\mathbb{R}$:

$$\vec{\sigma}(u_1, u_2) = \begin{pmatrix} x(u_1, u_2) \\ y(u_1, u_2) \\ z(u_1, u_2) \end{pmatrix}, \quad (u_1, u_2) \in D \subset \mathbb{R}^2 \,. \tag{2.1}$$

Each of these functions from $D \to \mathbb{R}$ is called a coordinate function. We shall use the notation above, i.e. x, y, z, but also σ_k, $k = 1, 2, 3$.

The first fundamental form of a surface describes how lengths and areas behave on the surface. Information about the Gaussian curvature of the surface can also be recovered from the first fundamental form. The first fundamental form is an intrinsic property of the surface, that is to say it is invariant under isometric deformations of the surface.

Definition 2 (First Fundamental Form)**.** The *first fundamental form* of a surface is given by:

$$g_{ij} = \frac{\partial \vec{\sigma}}{\partial u_i} \cdot \frac{\partial \vec{\sigma}}{\partial u_j}, \quad i, j = 1, 2 \,. \tag{2.2}$$

This now gives us a way of calculating the area of a patch of our surface directly from $\vec{\sigma}$ itself, which will be very useful when we come to minimising the area. A patch is the image of any subset of our domain, and we can calculate its area using the following:

$$A(\Sigma) = \iint_{\Delta} \sqrt{\det g_{ij}} \; du_1 \; du_2 \tag{2.3}$$

where Σ is the image of Δ under the surface mapping.

Definition 3 (Regular)**.** We describe a surface as *regular* if the determinant first fundamental form, $\det g_{ij} \neq 0$ for all points on the surface. Equivalently, surfaces are regular at a point when the coordinate tangent vectors are linearly independent, and hence the tangent plane is well defined.

In general it possible to reparameterise all surfaces such that they are regular, therefore, we shall assume all of our surfaces are regular.

Definition 4 (Unit Normal)**.** A *unit normal*, $\vec{N}$, of a surface at the point $p = (u_1, u_2)$ is a unit vector which is perpendicular to the tangent plane at that point. We shall use the unit normal which is computed as follows:

$$\vec{N}(u_1, u_2) = \left. \frac{\frac{\partial \vec{\sigma}}{\partial u_1} \times \frac{\partial \vec{\sigma}}{\partial u_2}}{\left\| \frac{\partial \vec{\sigma}}{\partial u_1} \times \frac{\partial \vec{\sigma}}{\partial u_2} \right\|} \right|_p . \tag{2.4}$$

Notice the cross product, $\times$, depends on the choice of orientation of $\mathbb{R}^3$, in that changing the orientation results in a change of sign of N.

Definition 5 (Second Fundamental Form)**.** The *second fundamental form* of a surface $\vec{\sigma}$, is given by:

$$b_{ij} = \frac{\partial^2 \vec{\sigma}}{\partial u_i \partial u_j} \cdot \vec{N}, \quad i, j = 1, 2 . \tag{2.5}$$

The second fundamental form encodes extrinsic information about the surface and how it is embedded in the ambient space, which in our case is $\mathbb{R}^3$, however it is possible to define minimal surfaces in other spaces [6]. The mean curvature is also an extrinsic property, unlike the Gaussian curvature, and hence is calculated using the second fundamental form. Using both the first and second fundamental forms we can get a succinct expression for the trace of the second fundamental form at a point on any surface.

Definition 6 (Mean Curvature)**.** Given a surface, $\vec{\sigma} \in \mathbb{R}^3$, then its *mean curvature* is defined as the trace of the second fundamental form, which is given in general by:

$$H(u_1, u_2) = \frac{g_{11}b_{22} + g_{22}b_{11} - 2g_{12}b_{12}}{2\det(g_{ij})} . \tag{2.6}$$

Geometrically, the mean curvature at a point p, on the surface is the sum of the two principal curvatures at that point. We can get the principal curvatures by considering the planes passing through the point p and containing the unit normal. As we can use the normal as an axis to rotate around there are an infinite number of such planes. The intersection of each of these planes and the surface is a path $\gamma : (\varepsilon, \varepsilon) \to \mathbb{R}^3$, with $\gamma(0) = p$. We can now take the curvature of this path as a plane curve, with the principal curvatures being the maximum and minimum curvatures that one can obtain in such a way.

With these elementary tools established we can give a more femoral definition of a minimal surface.

Definition 7 (Minimal Surface)**.** A *minimal surface* is a surface which has $H(u_1, u_2) = 0$ for all $u_1, u_2 \in D$.

We shall in the next section justify this definition of a minimal surface by looking at minimal surfaces as critical points of the area functional.

2.2 Minimal Surfaces by Variational Principle

In this section we shall use the variational principle to characterise minimal surfaces as critical points of the area functional. From this definition we can study properties of minimal surfaces and come up with a method of representing and generating them.

We shall begin by taking a surface and considering small local deformations. These small deformations will show us the properties required by a surface for it to be a critical point.

Let us take a surface $\vec{\sigma} : D \to \mathbb{R}^3$ and consider variations of the surface that are normal to it:

$$\vec{\sigma}_\lambda(u_1, u_2) = \vec{\sigma}(u_1, u_2) + \lambda h(u_1, u_2)\vec{N}(u_1, u_2)\,. \tag{2.7}$$

where h is a continuous and differentiable function with compact support, this is to say $h \in C_0^1(D)$. We require that h is zero outside of a compactly supported subset of D otherwise we would be considering global deformations of the surface, which could be not well defined for any $|\lambda| > 0$. The requirement that h is continuous and differentiable ensures that the surface generated by the deformation is also continuous and differentiable for $|\lambda| < \varepsilon,\ \varepsilon > 0$, and thus still has a well defined first fundamental form with which we can compute the area.

We are interested only in small changes of λ as this ensures the surface remains well defined. For example if we deform the surface such that the curvature increases there could be a value of λ such that an open set of the surface is mapped to a single point, thus we would no longer have a well defined surface.

We shall denote the first fundamental form of the surface obtained by a small deformation by $\tilde{g}_{ij}$. Denoting the area functional as:

$$A(\lambda) = \text{Area}(\vec{\sigma}_\lambda) = \iint_D \sqrt{\det \tilde{g}_{ij}}\; du_1 du_2 \tag{2.8}$$

the surface $\vec{\sigma}_0$ is said to be a critical point of the area functional iff $A'(0) = 0,\ \forall h \in C_0^1(\Omega)$.

Theorem 1. Minimal surfaces are critical points of the area functional.

Proof. We want to calculate the first fundamental form of a surface generated by a small deformation as in formula (2.7), so that we can calculate the area.

We note that $\frac{\partial \vec{\sigma}}{\partial u_i} \cdot \vec{N} = 0$ because $\frac{\partial \vec{\sigma}}{\partial u_i}$ lies in the tangent plane and $\vec{N}$ is by definition normal to this plane. We can then differentiate with respect to u_j giving $\frac{\partial^2 \vec{\sigma}}{\partial u_i \partial u_j} \cdot \vec{N} + \frac{\partial \vec{\sigma}}{\partial u_i} \cdot \frac{\partial \vec{N}}{\partial u_j} = 0$, by equation (2.5) we can see that $\frac{\partial^2 \vec{\sigma}}{\partial u_i \partial u_j} \cdot \vec{N} + \frac{\partial \vec{\sigma}}{\partial u_i} \cdot \frac{\partial \vec{N}}{\partial u_j} = b_{ij} + \frac{\partial \vec{\sigma}}{\partial u_i} \cdot \frac{\partial \vec{N}}{\partial u_j} = 0$, hence:

$$\frac{\partial \vec{\sigma}}{\partial u_i} \cdot \frac{\partial \vec{N}}{\partial u_j} = -b_{ij}\,. \tag{2.9}$$

We can calculate $\tilde{g}_{ij}$ by substituting the definition of $\vec{\sigma}\lambda$ into the equation for the first fundamental form, (2.2):

$$\tilde{g}_{ij} = \frac{\partial(\vec{\sigma} + \lambda h\vec{N})}{\partial u_i} \cdot \frac{\partial(\vec{\sigma} + \lambda h\vec{N})}{\partial u_j} \,. \tag{2.10}$$

By the linearity of differentiation we can see that:

$$\tilde{g}_{ij} = \left(\frac{\partial\vec{\sigma}}{\partial u_i} + \lambda\frac{\partial h}{\partial u_i}\vec{N} + \lambda h\frac{\partial\vec{N}}{\partial u_i}\right) \cdot \left(\frac{\partial\vec{\sigma}}{\partial u_j} + \lambda\frac{\partial h}{\partial u_j}\vec{N} + \lambda h\frac{\partial\vec{N}}{\partial u_j}\right) \tag{2.11}$$

$$= g_{ij} + \lambda h\frac{\partial\vec{\sigma}}{\partial u_i} \cdot \frac{\partial\vec{N}}{\partial u_j} + \lambda h\frac{\partial\vec{\sigma}}{\partial u_j} \cdot \frac{\partial\vec{N}}{\partial u_i} + \mathcal{O}(\lambda^2) \,. \tag{2.12}$$

Now we can use equation (2.9) to see that this then becomes:

$$\tilde{g}_{ij} = g_{ij} - 2\lambda h b_{ij} + \mathcal{O}(\lambda^2) \,. \tag{2.13}$$

Areas are calculated using $\det\tilde{g}_{ij}$, so we need to find an expression for this quantity.

$$\det\tilde{g}_{ij} = \det g_{ij} - 2\lambda h b_{11}g_{22} - 2\lambda h b_{22}g_{11} + 4\lambda h b_{12}g_{12} + \mathcal{O}(\lambda^2) \tag{2.14}$$

$$= \det g_{ij} - 4H\lambda h \det g_{ij} + \mathcal{O}(\lambda^2) \,. \tag{2.15}$$

From this we can indeed write down the full area functional explicitly in terms of an integral over the surface.

$$A(\lambda) = \iint \sqrt{\det g_{ij} - 4\lambda H(u_1,u_2)h(u_1,u_2)\det g_{ij} + \mathcal{O}(\lambda^2)}\; du_1 du_2 \,. \tag{2.16}$$

To find critical points we take the derivative with respect to λ.

$$A'(\lambda) = \frac{\partial}{\partial\lambda}\iint \sqrt{\det g_{ij} - 4\lambda H(u_1,u_2)h(u_1,u_2)\det g_{ij} + \mathcal{O}(\lambda^2)}\; du_1 du_2 \tag{2.17}$$

$$= \iint \frac{-4H(u_1,u_2)h(u_1,u_2)\det g_{ij} + \mathcal{O}(\lambda)}{2\sqrt{\det g_{ij} - 4\lambda H(u_1,u_2)h(u_1,u_2)\det g_{ij} + \mathcal{O}(\lambda^2)}}\; du_1 du_2 \,. \tag{2.18}$$

Now we are interested in making this a critical point when $\lambda = 0$.

$$A'(0) = \iint \frac{-2H(u_1,u_2)h(u_1,u_2)\det g_{ij}}{\sqrt{\det g_{ij}}}\; du_1 du_2 \tag{2.19}$$

$$= \iint -2H(u_1,u_2)h(u_1,u_2)\sqrt{\det g_{ij}}\; du_1 du_2 \,. \tag{2.20}$$

We are interested in the nature of critical points, characterised by $A'(0) = 0$, and so we set the above equation equal to zero:

$$0 = \iint -2H(u_1,u_2)h(u_1,u_2)\sqrt{\det g_{ij}}\; du_1 du_2 \,. \tag{2.21}$$

Following a standard argument in calculus of variations, if (2.21) holds for all $h \in C_0^1(D)$ then we have the following:

$$H(u_1,u_2) = 0 \,. \tag{2.22}$$

$\square$

This is an amazing result, the area of the surface, which is defined intrinsically, is linked with the mean curvature, which is an extrinsic property. Using this fact we can now study surfaces with zero mean curvature as this ensures they are critical points of the area functional and therefore minimal surfaces.

In this section we have looked at finding surfaces which are critical points of the area functional, however this does not necessarily mean they are area minimising, in the same fashion that critical points of a function are not necessarily minima. Nonetheless, minimal surfaces are locally area-minimising, i.e. given a point in a minimal surface, there exists a neighbourhood, U, which has less area than any other surface with the same boundary ∂U.

Next we shall show how minimal surfaces link to complex analysis.

3 Minimal Surfaces and Holomorphic Functions

In this section we shall use the foundations laid down in section 2 to make the link between minimal surfaces and complex analysis. This unification between minimal surfaces and complex analysis will give us the tools necessary to describe minimal surfaces in a more fundamental way.

3.1 Isothermal Parameters

In this section we shall look at isothermal parameters, including the definition, and some consequences and properties of this.

Definition 8 (Isothermal Parameters)**.** A surface is parametrised *isothermally* when the first fundamental form takes the special form:

$$g_{ij} = \lambda^2(u_1, u_2)\delta_{ij} \ , \tag{3.1}$$

where $\lambda(u_1, u_2)$ is some strictly positive function.

Theorem 2 (Isothermal mappings conserve angles)**.** Let us take two paths in our domain defined as γ_1 and γ_2 such that $\gamma_i : \mathbb{R} \to \mathbb{R}^2$, we can then compose them with $\vec{\sigma}$ and calculate the angles between the two tangent vectors of the surface.

Proof. Let us define the path on the surface as $\tilde{\gamma} = \sigma \circ \gamma$, then we can calculate the tangent vector of the path in the surface as follows:

$$\dot{\tilde{\gamma}} = \dot{\gamma}^1 \frac{\partial \vec{\sigma}}{\partial u_1} + \dot{\gamma}^2 \frac{\partial \vec{\sigma}}{\partial u_2} \ . \tag{3.2}$$

So to calculate the angle between these two vectors we take the inner product of the tangent vectors:

$$\frac{\partial}{\partial t}\vec{\sigma}(\vec{\gamma}_1)\cdot\frac{\partial}{\partial t}\vec{\sigma}(\vec{\gamma}_2) = (\dot{\gamma}_1^1\frac{\partial\vec{\sigma}}{\partial u_1} + \dot{\gamma}_1^2\frac{\partial\vec{\sigma}}{\partial u_2})\cdot(\dot{\gamma}_2^1\frac{\partial\vec{\sigma}}{\partial u_1} + \dot{\gamma}_2^2\frac{\partial\vec{\sigma}}{\partial u_2}) \tag{3.3}$$

$$= \dot{\gamma}_1^1\dot{\gamma}_1^2\frac{\partial\vec{\sigma}}{\partial u_1}\cdot\frac{\partial\vec{\sigma}}{\partial u_1} + \dot{\gamma}_1^1\dot{\gamma}_2^2\frac{\partial\vec{\sigma}}{\partial u_1}\cdot\frac{\partial\vec{\sigma}}{\partial u_2} + \dot{\gamma}_2^1\dot{\gamma}_1^2\frac{\partial\vec{\sigma}}{\partial u_1}\cdot\frac{\partial\vec{\sigma}}{\partial u_2} + \dot{\gamma}_2^1\dot{\gamma}_2^2\frac{\partial\vec{\sigma}}{\partial u_2}\cdot\frac{\partial\vec{\sigma}}{\partial u_2}\,. \tag{3.4}$$

Using the fact that the first fundamental form is given by $g_{ij} = \frac{\partial\vec{\sigma}}{\partial u_i}\cdot\frac{\partial\vec{\sigma}}{\partial u_j}$ we can substitute this in to equation 3.4 to get:

$$\frac{\partial}{\partial t}\vec{\sigma}(\vec{\gamma}_1)\cdot\frac{\partial}{\partial t}\vec{\sigma}(\vec{\gamma}_2) = \dot{\gamma}_1^1\dot{\gamma}_1^2 g_{11} + \dot{\gamma}_1^1\dot{\gamma}_2^2 g_{12} + \dot{\gamma}_2^1\dot{\gamma}_1^2 g_{12} + \dot{\gamma}_2^1\dot{\gamma}_2^2 g_{22}\,. \tag{3.5}$$

As we know our first fundamental form is given by $\lambda^2\delta_{ij}$ we can simplify the above to:

$$\frac{\partial}{\partial t}\vec{\sigma}(\vec{\gamma}_1)\cdot\frac{\partial}{\partial t}\vec{\sigma}(\vec{\gamma}_2) = \lambda^2(\dot{\gamma}_1^1\dot{\gamma}_1^2 + \dot{\gamma}_2^1\dot{\gamma}_2^2) = \lambda^2\dot{\gamma}_1\cdot\dot{\gamma}_2 \tag{3.6}$$

We can also see from the above that the norm of $\frac{\partial}{\partial t}\vec{\sigma}(\vec{\gamma})$ is given by $\lambda|\vec{\gamma}|$, and hence the cosine of the angle between the two vectors is given by:

$$\cos(\theta) = \frac{\lambda^2(\dot{\gamma}_1^1\dot{\gamma}_1^2 + \dot{\gamma}_2^1\dot{\gamma}_2^2)}{\lambda|\vec{\gamma}_1|\lambda|\vec{\gamma}_2|} = \frac{\dot{\gamma}_1^1\dot{\gamma}_1^2 + \dot{\gamma}_2^1\dot{\gamma}_2^2}{|\vec{\gamma}_1||\vec{\gamma}_2|} \tag{3.7}$$

Hence the angle is the same between the two tangent vectors of the paths in the surface is the same as the angle between the tangent vectors of the paths in the domain. □

The geometric intuition behind isothermal parameterisations is that $\vec{\sigma}$ preserves the angles between paths.

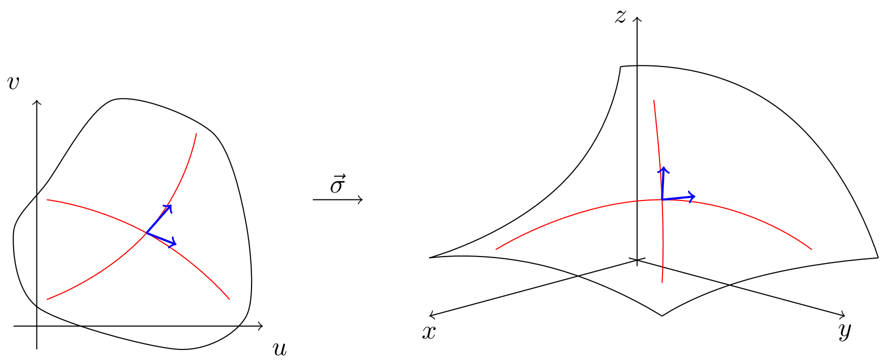

Figure 2: On the left we have our domain, with two paths. On the right is the image of $\vec{\sigma}$ and the image of the two paths. If $\vec{\sigma}$ is parameterised isothermally the angle between the two tangent vectors of the paths in the domain must equal the angle between the two tangent vectors of the paths in the image.

In order to show the existence of isothermal parameters for minimal surfaces, we will need the following lemma, taken from [7] which is a result in the field of differential geometry:

Lemma 1 (Poincaré)**.** On says that on a contractible manifold, all closed forms are exact.

In the context we require for our proof we can interpret this as saying, if we have two functions, $f : \mathbb{R}^2 \to \mathbb{R}$ and $g : \mathbb{R}^2 \to \mathbb{R}$, such that $\frac{\partial f}{\partial x} = \frac{\partial g}{\partial y}$ and $\frac{\partial f}{\partial y} = \frac{\partial g}{\partial x}$ then there exists a function $h : \mathbb{R}^2 \to \mathbb{R}$, such that $f = \frac{\partial h}{\partial x}$ and $g = \frac{\partial h}{\partial y}$.

Theorem 3 (Isothermal Parameters)**.** It is always possible to find an *isothermal parametrisation* in a small neighbourhood of a regular point p of a minimal surface $\vec{\sigma}$.

We base the structure of our proof on the one given in [8] §4

Proof. We know that it is possible to express a small enough simply connected neighbourhood around a regular point of a surface as a graph over the tangent plane, i.e. there exists a rigid motion of the entire surface which then allows us to express it locally as $z = f(u_1, u_2)$. If we switch to this parametrization, we get

$$\vec{\sigma} = \begin{pmatrix} u_1 \\ u_2 \\ f(u_1, u_2) \end{pmatrix} \quad \Longrightarrow \quad \frac{\partial \vec{\sigma}}{\partial u_1} = \begin{pmatrix} 1 \\ 0 \\ \frac{\partial f}{\partial u_1} \end{pmatrix}, \quad \frac{\partial \vec{\sigma}}{\partial u_2} = \begin{pmatrix} 0 \\ 1 \\ \frac{\partial f}{\partial u_2} \end{pmatrix} \tag{3.8}$$

In order to make the calculations easier to read we shall use the following notation:

$$p = \frac{\partial f}{\partial u_1}, \qquad q = \frac{\partial f}{\partial u_2}, \tag{3.9}$$

$$r = \frac{\partial^2 f}{\partial {u_1}^2}, \qquad s = \frac{\partial^2 f}{\partial u_1 \partial u_2}, \qquad t = \frac{\partial^2 f}{\partial {u_2}^2}\,. \tag{3.10}$$

Using equations (3.9) we can see that the first fundamental form of the surface can be expressed using p and q:

$$g_{ij} = \begin{pmatrix} 1 + p^2 & pq \\ pq & 1 + q^2 \end{pmatrix}, \tag{3.11}$$

and let $W = \sqrt{\det g_{ij}}$. It is possible to show that these functions below satisfy the requirements for lemma 1, and hence there exists two functions $F(u_1, u_2)$ and $G(u_1, u_2)$ which satisfy the following relations:

$$\frac{\partial F}{\partial u_1} = \frac{1+p^2}{W}, \qquad \frac{\partial F}{\partial u_2} = \frac{pq}{W}, \tag{3.12}$$

$$\frac{\partial G}{\partial u_1} = \frac{pq}{W}, \qquad \frac{\partial G}{\partial u_2} = \frac{1+q^2}{W}\,. \tag{3.13}$$

If we then construct a new set of coordinates, ξ_1 and ξ_2 such that $\xi_1 = u_1 + F(u_1, u_2)$ and $\xi_2 = u_2 + G(u_1, u_2)$, we can then calculate the Jacobian of the transformation from (u_1, u_2) to (ξ_1, ξ_2).

$$J = \frac{\partial(\xi_1, \xi_2)}{\partial(u_1, u_2)} = \begin{pmatrix} 1 + \frac{1+p^2}{W} & \frac{pq}{W} \\ \frac{pq}{W} & 1 + \frac{1+q^2}{W} \end{pmatrix} \tag{3.14}$$

In order to be able to invert this coordinate transform we need $\det J = |J| > 0$, but

$$\det J = \left(1 + \frac{1+p^2}{W}\right)\left(1 + \frac{1+q^2}{W}\right) - \left(\frac{pq}{W}\right)^2 \tag{3.15}$$

$$= 1 + \frac{2+p^2+q^2}{W} + \frac{1+p^2+q^2}{W^2} \tag{3.16}$$

$$= 2 + \frac{2+p^2+q^2}{W} \tag{3.17}$$

$$> 0\,. \tag{3.18}$$

Thus this transformation has a local inverse, so we can express the surface in terms of these coordinates. By inverting this matrix we get

$$J^{-1} = \frac{1}{|J|W} \begin{pmatrix} W+1+q^2 & -pq \\ -pq & W+1+p^2 \end{pmatrix} . \tag{3.19}$$

Now, by the chain rule we get $\frac{\partial \vec{\sigma}}{\partial \xi_1} = \frac{\partial \vec{\sigma}}{\partial u_1}\frac{\partial u_1}{\partial \xi_1} + \frac{\partial \vec{\sigma}}{\partial u_2}\frac{\partial u_2}{\partial \xi_1}$ and from this we can see that

$$\frac{\partial \vec{\sigma}}{\partial \xi_1} = \frac{1}{|J|W} \begin{pmatrix} W+1+q^2 \\ -pq \\ p(W+1+q^2)-q(pq) \end{pmatrix}, \quad \frac{\partial \vec{\sigma}}{\partial \xi_2} = \frac{1}{|J|W} \begin{pmatrix} -pq \\ W+1+p^2 \\ -p(pq)+q(W+1+p^2) \end{pmatrix}, \tag{3.20}$$

Now our first fundamental form is simply given by the inner product of these vectors, i.e.:

$$\tilde{g}_{11} = \frac{\partial \vec{\sigma}}{\partial \xi_1} \cdot \frac{\partial \vec{\sigma}}{\partial \xi_1} = \frac{1}{|J|^2 W^2} \begin{pmatrix} W+1+q^2 \\ -pq \\ p(W+1+q^2)-q(pq) \end{pmatrix} \cdot \begin{pmatrix} W+1+q^2 \\ -pq \\ p(W+1+q^2)-q(pq) \end{pmatrix}, \tag{3.21}$$

$$\tilde{g}_{22} = \frac{\partial \vec{\sigma}}{\partial \xi_2} \cdot \frac{\partial \vec{\sigma}}{\partial \xi_2} = \frac{1}{|J|^2 W^2} \begin{pmatrix} -pq \\ W+1+p^2 \\ -p(pq)+q(W+1+p^2) \end{pmatrix} \cdot \begin{pmatrix} -pq \\ W+1+p^2 \\ -p(pq)+q(W+1+p^2) \end{pmatrix}, \tag{3.22}$$

$$\tilde{g}_{12} = \frac{\partial \vec{\sigma}}{\partial \xi_1} \cdot \frac{\partial \vec{\sigma}}{\partial \xi_1} = \frac{1}{|J|^2 W^2} \begin{pmatrix} W+1+q^2 \\ -pq \\ p(W+1+q^2)-q(pq) \end{pmatrix} \cdot \begin{pmatrix} -pq \\ W+1+p^2 \\ -p(pq)+q(W+1+p^2) \end{pmatrix}. \tag{3.23}$$

We now only require some simple (but long) algebra to show that $\tilde{g}_{11} = \tilde{g}_{22}$, and $\tilde{g}_{12} = \tilde{g}_{21} = 0$. □

Using the the fact that $g_{ij} = \lambda^2 \delta_{ij}$ we can now simplify many of the equations for the properties of the minimal surface. For example, the determinant of the first fundamental form is given by $\det g_{ij} = \lambda^4$, and from this we can see that the mean curvature can now be written as:

$$H = \frac{b_{11} + b_{22}}{2\lambda^2} \tag{3.24}$$

There is a more general proof to show that, in fact, any surface can be parameterised isothermally. However, we have been able to leverage some of the properties of minimal surfaces to show this in a much simpler way.

3.2 Surface Laplacian

In this section we shall study the surface Laplace–Beltrami operator defined on the surface, we shall often shorten this to just the Laplacian of the surface.

The Laplacian of a function defined on a surface is given, in general coordinates, as:

$$\Delta^\sigma f(u_1, u_2) := \sum_{i,j=1}^{2} \frac{1}{\sqrt{\det g}} \frac{\partial}{\partial u_i} \left(\sqrt{\det g}\, g_{ij} \frac{\partial}{\partial u_j} f(u_1, u_2) \right) . \tag{3.25}$$

Because we can parameterise minimal surfaces iosthermally we can simply take a multiple of the traditional, planar Laplacian of the coordinate functions, given by, $\Delta^\sigma x(u_1, u_2) = \frac{1}{\lambda^2}\frac{\partial^2 x}{\partial {u_1}^2} + \frac{1}{\lambda^2}\frac{\partial^2 x}{\partial {u_2}^2}$ in these isothermal coordinates. We also note the Laplacian of a vector-valued function is simply the vector of the Laplacian of each of these functions. From here we see that the Laplacian of the surface vector itself is given by:

$$\Delta^\sigma \vec{\sigma} = \frac{1}{\lambda^2}(\Delta x, \Delta y, \Delta z)\,. \tag{3.26}$$

If we have a surface which is parameterised isothermally we can say that

$$\frac{\partial \vec{\sigma}}{\partial u_1} \cdot \frac{\partial \vec{\sigma}}{\partial u_1} = \frac{\partial \vec{\sigma}}{\partial u_2} \cdot \frac{\partial \vec{\sigma}}{\partial u_2}, \tag{3.27}$$

$$\frac{\partial \vec{\sigma}}{\partial u_1} \cdot \frac{\partial \vec{\sigma}}{\partial u_2} = 0\,. \tag{3.28}$$

Differentiating (3.27) with respect to u_1 we get:

$$\frac{\partial \vec{\sigma}}{\partial u_1} \cdot \frac{\partial^2 \vec{\sigma}}{\partial {u_1}^2} = \frac{\partial \vec{\sigma}}{\partial u_2} \cdot \frac{\partial^2 \vec{\sigma}}{\partial u_1 \partial u_2}\,, \tag{3.29}$$

and differentiating (3.28) with respect to u_2:

$$\frac{\partial^2 \vec{\sigma}}{\partial u_1 \partial u_2} \cdot \frac{\partial \vec{\sigma}}{\partial u_2} = -\frac{\partial \vec{\sigma}}{\partial u_1} \cdot \frac{\partial^2 \vec{\sigma}}{\partial {u_2}^2}\,. \tag{3.30}$$

From this we can see that:

$$\frac{\partial \vec{\sigma}}{\partial u_1} \cdot \underbrace{\left(\frac{\partial^2 \vec{\sigma}}{\partial {u_1}^2} + \frac{\partial^2 \vec{\sigma}}{\partial {u_2}^2}\right)}_{=\lambda^2 \Delta^\sigma \vec{\sigma}} = 0\,. \tag{3.31}$$

As we have taken our surface to be regular we know that $\lambda^2 \neq 0$ and hence this shows that $\Delta^\sigma \vec{\sigma}$ is orthogonal to the tangent vector given by $\frac{\partial \vec{\sigma}}{\partial u_1}$. We can then also differentiate (3.27) with respect to u_2 and (3.28) with respect to u_1 to get $\frac{\partial \vec{\sigma}}{\partial u_2} \cdot \Delta^\sigma \vec{\sigma} = 0$ via exactly the same argument. We have now shown that $\Delta^\sigma \vec{\sigma}$ is perpendicular to both tangent vectors, which are lineally independent and span the tangent plane of the surface, and hence we have $\Delta^\sigma \vec{\sigma} \parallel \vec{N}$.

If we consider $\Delta \vec{\sigma} \cdot \vec{N}$ and use the second fundamental form we can see that

$$\Delta^\sigma \vec{\sigma} \cdot \vec{N} = \frac{1}{\lambda^2}\frac{\partial^2 \vec{\sigma}}{\partial {u_1}^2} \cdot \vec{N} + \frac{1}{\lambda^2}\frac{\partial^2 \vec{\sigma}}{\partial {u_2}^2} \cdot \vec{N} = \frac{b_{11} + b_{22}}{\lambda^2} = 2H\,. \tag{3.32}$$

We shall describe a function which satisfies the equation $\Delta f(x, y) = 0$ as harmonic. This leads us to the following proposition.

Proposition 1 (Minimal surfaces have harmonic coordinate functions)**.** *Proof.* Let $\vec{\sigma}$ be a surface parametrised isothermally. We have shown that $\Delta^\sigma \vec{\sigma} \cdot \vec{N} = 2\lambda^2 H$. We also know that $\vec{\sigma}$ is minimal $\iff$ $H = 0$, it is easy to see that this is indeed the case when $\Delta^\sigma \vec{\sigma} = 0$. The normal vector $\vec{N}$ is never the zero vector as it has, by definition, unit length, and λ^2 is never zero as we made the assumption that all surfaces are parameterised such that they are regular. Hence we can see that, $\vec{\sigma}$ is minimal $\iff H = 0 \iff \Delta^\sigma \vec{\sigma} = 0 \iff \Delta x = \Delta y = \Delta z = 0$. □

The structure of minimal surfaces not only allows us to find isothermal parameters in any small enough neighbourhood, but also tells us that once we have done so the coordinate functions will be harmonic. We now have a new way of describing minimal surfaces based solely on the coordinate functions, and from this we can explore ways of finding such coordinate functions.

In the next section we shall look at how to incorporate these two conditions into one representation for minimal surfaces.

3.3 Harmonic and Holomorphic Functions

As shown in the previous section, we can study parametric surfaces whose components are harmonic and are parametrised isothermally. Thus we have two conditions on $\vec{\sigma}$ for it to be isothermal, the two equations stated in the previous section (3.27) and (3.28). We can combine these into one statement by multiplying (3.28) by $2i$, so we get one equation, but in complex variables:

$$\sum_{k=1}^{3}\left[\left(\frac{\partial \sigma_k}{\partial u_1}\right)^2 - \left(\frac{\partial \sigma_k}{\partial u_2}\right)^2 - 2i\frac{\partial \sigma_k}{\partial u_1}\frac{\partial \sigma_k}{\partial u_2}\right] = 0\,. \tag{3.33}$$

The advantage of using complex numbers is that we can then factorise equation 3.33 like so:

$$\sum_{k=1}^{3}\left(\frac{\partial \sigma_k}{\partial u_1} - i\frac{\partial \sigma_k}{\partial u_2}\right)^2 = 0\,. \tag{3.34}$$

This is a useful way of talking about the surface, so we shall label the components of the expression inside the brackets of the above equation. Let us say $\phi_k(z) = \frac{\partial \sigma_k}{\partial u_1} - i\frac{\partial \sigma_k}{\partial u_2}$ where $z = u_1 + iu_2$.

Also, let us recall the Cauchy-Riemann equations for a holomorphic function in the form $f(u,v) = a(u,v) + ib(u,v)$, where a and b are functions $\mathbb{R}^2 \to \mathbb{R}$, are:

$$\frac{\partial a}{\partial u} = \frac{\partial b}{\partial v}, \tag{3.35}$$

$$\frac{\partial a}{\partial v} = -\frac{\partial b}{\partial u}\,. \tag{3.36}$$

We note that the ϕ_k functions are indeed of this form, with $a = \frac{\partial \sigma_k}{\partial u_1}$ and $b = -\frac{\partial \sigma_k}{\partial u_2}$, and when we look at the first Cauchy-Riemann equation, (3.35), with these functions we obtain:

$$\frac{\partial^2 \sigma_k}{\partial {u_1}^2} = -\frac{\partial^2 \sigma_k}{\partial {u_2}^2}, \tag{3.37}$$

$$\implies \frac{\partial^2 \sigma_k}{\partial {u_1}^2} + \frac{\partial^2 \sigma_k}{\partial {u_2}^2} = 0\,. \tag{3.38}$$

For (3.36) to be satisfied we simply require $\frac{\partial^2 \sigma_k}{\partial u_1 \partial u_2} = \frac{\partial^2 \sigma_k}{\partial u_2 \partial u_1}$ which follows from Clairaut's Theorem (also known as Schwarz's Theorem) as found in [10] which states:

Theorem 4 (Clairout's Theorem)**.** If $f : \mathbb{R}^2 \to \mathbb{R}$ has continuous second partial derivatives at any point, then these derivatives in fact commute.

From this we can conclude that if σ_k is harmonic then ϕ_k will be holomorphic.

It is interesting to see that if we are only given the ϕ_k functions we can recover the surface up to a translation, which we shall now show. We can see that, by the Cauchy-Riemann equations,

$$\vec{\phi}(u_1, u_2) = \frac{\partial \vec{\sigma}}{\partial u_1} - i\frac{\partial \vec{\sigma}}{\partial u_2} = \frac{\partial \vec{\sigma}}{\partial u_1} + i\frac{\partial \vec{\sigma}}{\partial u_1} = \vec{\Phi}(u_1, u_2), \tag{3.39}$$

i.e. ϕ_k is the complex derivative of a holomorphic function Φ_k, where Φ_k is given by $\Phi_k(u,v) = \int_{x_0}^{u+iv} \phi_k(z)\ dz$, this is always unique and well defined as ϕ_k is holomorphic. Now $\Phi_k = \sigma_k(u,v) + i\sigma_k(u,v) + C$, for some constant $C \in \mathbb{C}$. Hence the surface is recovered up to a translation by taking $\sigma_k(u,v) = \Re\left[\int_{x_0}^{u+iv} \phi_k(z)\ dz + C\right]$, for each $k = 1, 2, 3$, where $\Re[z]$ signifies taking the real part of z. From now on if two surfaces are translations of each other, we can and shall consider them the same surface.

From this we can see that minimal surfaces can always be decomposed into three holomorphic functions, and conversely, three holomorphic functions whose square sum is 0 can be integrated to obtain a minimal surface. This is a powerful link between the study of minimal surfaces and that of complex analysis. This allows us to now use the language of complex analysis to describe and study minimal surfaces.

4 The Weierstrass Representation

In this section we shall look at the representation of minimal surfaces proposed by both Weierstrass and Enneper. The representation uses pairs of functions which can then be used to obtain the ϕ_k functions from section 3.3 in such a way that they fulfil the restrictions that they are holomorphic and their square sum vanishes.

Proposition 2 (Weierstrass Representation)**.** Every simply connected minimal surface can be generated from a pair of functions (f, g) where f is holomorphic and g is meromorphic, and at each pole of g, with order m, f has a zero of order $2m$. Conversely, any pair of functions (f, g) which satisfy the above holomorphicity conditions generates a minimal surface via the parameterisation:

$$\vec{\phi} = \begin{pmatrix} \frac{1}{2} f(1 - g^2) \\ \frac{i}{2} f(1 + g^2) \\ fg \end{pmatrix}, \tag{4.1}$$

Where f and g function given by.

$$f = \phi_1 - i\phi_2, \qquad g = \frac{\phi_3}{\phi_1 - i\phi_2}. \tag{4.2}$$

Proof. Let us start by showing every minimal surface can be generated from a pair of functions.

Let $\vec{\sigma}$ be a minimal surface parameterised isothermally, and let ϕ_k, $k = 1, 2, 3$, be the diffentials of the surface as defined in the previous section. Then we know that each ϕ_k is holomorphic, and they satisfy the equation:

$$\phi_1{}^2 + \phi_2{}^2 + \phi_3{}^2 = 0. \tag{4.3}$$

From here we can again use complex numbers to factorise this equation into smaller parts:

$$\phi_1{}^2 + \phi_2{}^2 = -\phi_3{}^2, \tag{4.4}$$

$$(\phi_1 - i\phi_2)(\phi_1 + i\phi_2) = -\phi_3{}^2 . \tag{4.5}$$

If we denote $\phi_1 - i\phi_2 = f$, then we know that f will be a holomorphic function, and let $g = \frac{\phi_3}{\phi_1 - i\phi_2} = \frac{\phi_3}{f}$ then g will be meromorhphic, with a pole at each point where f has a zero. We can now indeed recover the ϕ_k functions from f and g. We can easily see that $fg = \phi_3$, and so:

$$f(1-g^2) = (\phi_1 - i\phi_2)\left(1 - \frac{\phi_3^2}{(\phi_1 - i\phi_2)^2}\right) \tag{4.6}$$

$$= \phi_1 - i\phi_2 - \frac{\phi_3^2}{\phi_1 - i\phi_2} . \tag{4.7}$$

By equation (4.5) we can then see:

$$f(1-g^2) = \phi_1 - i\phi_2 + \phi_1 + i\phi_2 = 2\phi_1 . \tag{4.8}$$

Similarly we can compute $f(1+g^2) = -2i\phi_2$, and hence we find:

$$\vec{\phi} = \begin{pmatrix} \frac{1}{2}f(1-g^2) \\ \frac{i}{2}f(1+g^2) \\ fg \end{pmatrix} . \tag{4.9}$$

And hence the surface can be recovered from (f, g).

Now we need to show that given a pair of functions (f, g), that these do indeed produce a minimal surface.

We need to check that the functions produced via the parameterisation (4.1) do indeed satisfy the conditions set on $\vec{\phi}$, namely that the sum over $\phi_k^2 = 0$ and that each ϕ_k is holomorphic.

Firstly, we see that each ϕ_k is indeed holomorphic as f is holomorphic by assumption and any pole in g is paired with a zero in f of twice the order. Hence when we multiply f with g^2 no poles remain and the function is holomorphic.

Next we can check that the square sum is zero by a simple calculation:

$$\sum_{k=1}^{3} \phi_k{}^2 = \left(\frac{1}{2}f(1-g^2)\right)^2 + \left(\frac{i}{2}f(1+g^2)\right)^2 + (fg)^2 \tag{4.10}$$

$$= \frac{1}{4}f^2 - \frac{1}{2}f^2g^2 + \frac{1}{4}f^2g^4 - \frac{1}{4}f^2 - \frac{1}{2}f^2g^2 - \frac{1}{4}f^2g^4 + f^2g^2 \tag{4.11}$$

$$= 0 . \tag{4.12}$$

And hence the pair (f, g) via the Weierstrass parameterisation does indeed produce a minimal surface. $\square$

This has shown there is a direct correspondence between minimal surfaces and suitable pairs of complex meromorphic functions. It is remarkable that putting constraints on the surface area of a surface has led us to pairs of complex functions. Through the unification of minimal surfaces and complex analysis we can get a deep insight into the behaviour and types of minimal surfaces and study them in a new context from which we can rapidly gain deeper understanding.

In the next section we shall look into the geometric significance behind the functions, f and g and show how intrinsically they are tied to the surface.

4.1 Weierstrass Data and the Stereographic Projection

In this section we seek to explore what information we can glean about a minimal surface directly from the Weierstrass representation. This is interesting as it allows us to explore geometric properties directly from not only complex, holomorphic and meromorphic functions, about which a lot of information is known due to the study of complex analysis.

As established in the previous section, a surface can be encoded in two functions, (f, g) using the Weierstrass reprsentation.

$$\vec{\phi} = \begin{pmatrix} \frac{1}{2}f(1-g^2) \\ \frac{i}{2}f(1+g^2) \\ fg \end{pmatrix}, \qquad \vec{\sigma} = \Re \int \vec{\phi}\, dz \tag{4.13}$$

We shall call the functions f and g the Weierstrass data for the surface $\vec{\sigma}$, as they contain all the information needed to reconstruct the surface.

4.2 The First Fundamental Form

Calculation of the first fundamental form is a straightforward process as the Weierstrass representation produces an isothermal parameterisation, and hence the first fundamental form is given by $g_{ij} = \lambda^2 \delta_{ij}$. Our aim is to calculate the conformal factor λ^2:

$$\lambda^2 = \left|\frac{\partial \vec{\sigma}}{\partial u_1}\right|^2 = \left|\frac{\partial \vec{\sigma}}{\partial u_2}\right|^2 \tag{4.14}$$

$$= \frac{1}{2}\left(\left|\frac{\partial \vec{\sigma}}{\partial u_1}\right|^2 + \left|\frac{\partial \vec{\sigma}}{\partial u_2}\right|^2\right) \tag{4.15}$$

$$= \frac{1}{2}\sum_{k=1}^{3} |\phi_k|^2 \tag{4.16}$$

$$= \left[\frac{|f|(1+|g|^2)}{2}\right]^2 \tag{4.17}$$

More importantly however we would like to calculate the unit normal of the surface, the formula for which is given in section 2. From this we can calculate the Gauss map of the surface in terms of f and g. Further details of this calculation can be found in Section 7 of [9]. The normal of the surface at a point is given by:

$$\hat{N}(u_1, u_2) = \frac{\partial \vec{\sigma}}{\partial u_1} \times \frac{\partial \vec{\sigma}}{\partial u_2} = \Im \begin{pmatrix} \phi_1 \bar{\phi}_2 \\ \phi_3 \bar{\phi}_1 \\ \phi_1 \bar{\phi}_2 \end{pmatrix}, \tag{4.18}$$

which after factoring out common parts gives:

$$N = \frac{|f|(1+|g|^2)}{4} \begin{pmatrix} 2\Re g \\ 2\Im g \\ |g|^2 - 1 \end{pmatrix}, \tag{4.19}$$

and hence from this we can calculate the Gauss Map of the surface:

$$N(u_1, u_2) = \frac{\frac{\partial \vec{\sigma}}{\partial u_1} \times \frac{\partial \vec{\sigma}}{\partial u_2}}{|\frac{\partial \vec{\sigma}}{\partial u_1} \times \frac{\partial \vec{\sigma}}{\partial u_2}|} = \begin{pmatrix} \frac{2\Re[g]}{|g|^2+1} \\ \frac{2\Im[g]}{|g|^2+1} \\ \frac{|g|^2-1}{|g|^2+1} \end{pmatrix} \in \mathbb{S}^2 . \tag{4.20}$$

Let us recall that the stereographic projection, ϕ, of a point in $\mathbb{C}$ into the sphere $\mathbb{S}^2$ with centre $(0, 0, \frac{1}{2})$ is:

$$\phi(z) = \begin{pmatrix} \frac{2\Re[z]}{|z|^2+1} \\ \frac{2\Im[z]}{|z|^2+1} \\ \frac{|z|^2+1}{|z|^2+1} \end{pmatrix}. \tag{4.21}$$

From the previous equation it is clear to see that the Gauss map is simply given by $\phi \circ g$. That is to say, the Gauss map coincides with the stereographic projection of the function g onto the unit sphere, i.e. we get the following commutative diagram.

$$\begin{tikzcd} \Sigma \arrow[r, "N"] & \mathbb{S}^2 \\ \Omega \arrow[u, "\vec{\sigma}"] \arrow[r, dotted, "g"] & \bar{\mathbb{C}} \arrow[u, "\phi"'] \end{tikzcd}$$

Figure 3: The relationship $\vec{N}$ and the Weierstrass function g.

It turns out that not only is the Weierstrass representation an easy way of encoding information about a minimal surface, it also gives us a lot of geometric insight into the properties of our surface. We did not set out to encode information about our surface in this way, however the fact that we do get this shows how intrinsically a surface is connected to its Weierstrass representation.

4.3 The Associate Family

In this section we shall look at associate families of minimal surfaces, which families of isometric minimal surfaces generated by a single parameter. This gives us a way to link seemingly unconnected surfaces into a single family.

The first fundamental form of a minimal surface with Weierstrass representation f and g, as given in equation (4.17) is:

$$g_{ij} = \left[\frac{|f|(1+|g|^2)}{2}\right]^2 \delta_{ij}\,. \tag{4.22}$$

Notice we can multiply f by any complex number, with modulus one, while still leaving (4.22) form invariant as it only depends on $|f|$. Using this we can generate families of isometric surfaces by parameterising the set of all complex numbers of unit length by $e^{i\theta}$, $\theta \in [0, 2\pi)$. From here we get:

$$\vec{\sigma}_\theta(u_1, u_2) = \Re\left[e^{i\theta}\int \begin{pmatrix} \frac{1}{2}f(1-g^2) \\ \frac{i}{2}f(1+g^2) \\ fg \end{pmatrix} dz\right]. \tag{4.23}$$

We call such a family of surfaces an associate family. We can view this family as a rotation of the image of f in the complex plane by the angle θ, noting that $\vec{\sigma}_0 = \vec{\sigma}_{2\pi}$. As shown in section 4.2 the Gauss map of the surface is dependent only on the function g and hence the Gauss map of such a family is unaffected by a change in θ.

Having such a powerful way of generating families of minimal surfaces we shall go on to study the shared properties of surfaces in this family.

First we can see, by construction, that the first fundamental form is the same for all surfaces in the family, and hence the surfaces are isometric. We also know that the Weierstrass representation generates a conformal mapping and hence angles between paths in the domain are equal to the angles between the paths generated in the surface, from this we can see that angles are also preserved for all surfaces in the family. So we have that, locally, distances and angles are preserved.

When θ takes on the values $\frac{\pi}{2}$, the real parts of f become imaginary and the imaginary parts become real. We call the surface generated at this specific value the *conjugate surface* of the one we obtain when $\theta = 0$.

The are many properties that can be learnt about the conjugate of a surface just by studying the surface itself.

The following theorem can be found on page 27 in [12].

Theorem 5 (Planes of symmetry correspond to lines)**.** If there exists a plane of symmetry for a given minimal surface, then the path defined by the intersection of the symmetry plane and the surface corresponds to a straight line in the conjugate surface.

Conversely straight lines embedded in the surface correspond to planar paths defining a plane of symmetry. Moreover the direction of the straight line is given by normal vector alone the plane path.

We shall now look at some canonical examples of minimal surfaces and how they are related via associate families.

5 A Survey of Minimal Surfaces

In this section we shall explore some examples of minimal surfaces in relation to their Weierstrass representations. We shall commence our survey by studying the Enneper surface, but we shall focus most of our attention on two canonical examples of minimal surfaces, the catenoid and helicoid.

Definition 9 (Embedded)**.** We call a surface embedded if it contains no self intersections.

Definition 10 (Complete)**.** A surface is complete if for all point p contained in the surface a geodesic in any direction is defined for all real value of its parameter.

For a long time it was thought that the plane, catenoid, and helicoid were the only complete minimal surfaces to be embedded in $\mathbb{R}^3$ of finite genus. In fact we shall see in the next section that the Costa surface is also embedded.

5.1 The Enneper Surface

The discovery of the Enneper surface signified an important step in the field of minimal surfaces as it was one of the first surfaces studied that was generated by the Weierstrass representation, and proved how powerful the representation is at producing new, previously unthought-of surfaces.

The representation for the Enneper surface is given by:

$$f(z) = 1, \qquad g(z) = z \ , \tag{5.1}$$

from whence we get the following:

$$\vec{\phi} = \begin{pmatrix} \frac{1}{2}(1 - z^2) \\ \frac{i}{2}(1 + z^2) \\ z \end{pmatrix} . \tag{5.2}$$

To calculate the equation for the surface we are required to integrate the components of (5.2). We shall consider each coordinate function individually, starting with the σ_1, for which we get the following expression:

$$\begin{aligned} \sigma_1(u_1, u_2) &= \Re\left[\int_0^{u_1+iu_2} \frac{1}{2}(1 - z^2)\, dz\right] \\ &= \Re\left[\left[\frac{1}{2}z - \frac{1}{6}z^3\right]_0^{u_1+iu_2}\right] \\ &= \Re\left[\frac{1}{2}(u_1 + iu_2) - \frac{1}{6}({u_1}^3 + 3i{u_1}^2 v - 3u_1{u_2}^2 - i{u_2}^3)\right] \\ &= \frac{1}{2}u_1 - \frac{1}{6}{u_1}^3 + \frac{1}{2}u_1{u_2}^2 \\ &= \frac{1}{2}u_1\left(1 - \frac{1}{3}{u_1}^2 + {u_2}^2\right) . \end{aligned} \tag{5.3}$$

For the second component we find:

$$
\begin{aligned}
\sigma_2(u_1,u_2) &= \Re\left[\int_0^{u_1+iu_2} \frac{1}{2}(1+z^2)\,dz\right] \\
&= \Re\left[\left[\frac{i}{1}z+\frac{i}{6}z^3\right]_0^{u_1+iu_2}\right] \\
&= \Re\left[\frac{i}{2}(u_1+iu_2)+\frac{i}{6}(u^3+3iu^2v-3uv^2-iv^3)\right] \\
&= -\frac{1}{2}u_2+\frac{1}{6}{u_2}^3-\frac{1}{2}{u_1}^2u_2 \\
&= -\frac{1}{2}u_2\left(1+\frac{1}{3}{u_2}^2-{u_1}^2\right).
\end{aligned}
\tag{5.4}
$$

And finally the last coordinate is given by:

$$
\begin{aligned}
\sigma_3(u_1,u_2) &= \Re\left[\int_0^{u_1+iu_2} z\,dz\right] \\
&= \Re\left[\left[\frac{1}{2}z^2\right]_0^{u_1+iu_2}\right] \\
&= \Re\left[{u_1}^2-{u_2}^2+2iu_1u_2\right] \\
&= \frac{1}{2}({u_1}^2-{u_2}^2).
\end{aligned}
\tag{5.5}
$$

Hence, combining the components we calculated in equations (5.3), (5.4), and (5.5) we find the final surface parameterisation is as follows:

$$
\vec{\sigma}(u_1,u_2) = \begin{pmatrix} \frac{1}{2}u_1(1-\frac{1}{3}{u_1}^2+{u_2}^2) \\ -\frac{1}{2}u_2(1-\frac{1}{3}{u_2}^2+{u_1}^2) \\ \frac{1}{2}({u_1}^2-{u_2}^2) \end{pmatrix}.
\tag{5.6}
$$

Now we have found the equation we can graph the surface, which can be found in figure 4.

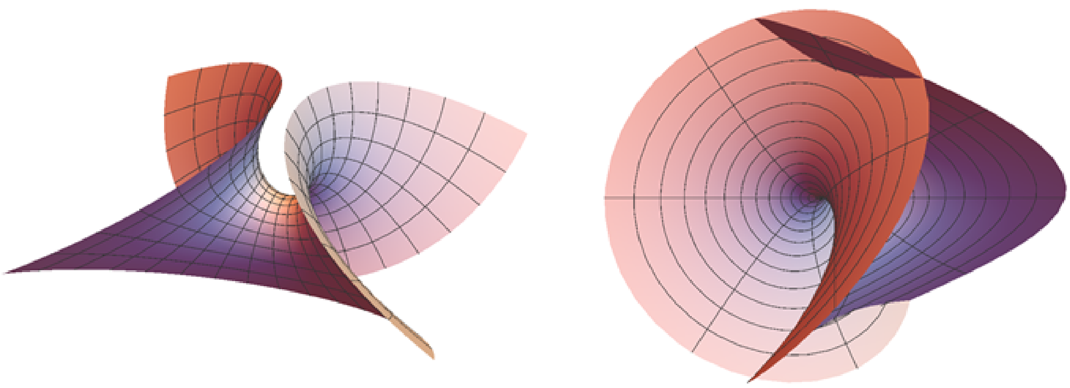

Figure 4: Two plots of the Enneper surface showing its shape. On the left is a plot of a small region of the Enneper surface near the origin. On the right is a plot of a larger section of the domain, as we can see, outside of a small region the surface is no longer embedded. The surface intersections are contained in the $x = 0$ and $y = 0$ planes.

An interesting property is the Enneper surface is that it is its own conjugate. If we take the conjugate surface which is given by the formula:

$$\vec{\sigma}(u_1, u_2) = \Re\left[\int i \begin{pmatrix} \frac{1}{2}(1-z^2) \\ \frac{i}{2}(1+z^2) \\ z \end{pmatrix} dz\right] , \tag{5.7}$$

we can then integrate to find the equation for the surface is:

$$= \begin{pmatrix} -\frac{1}{2}u_2\left(1+\frac{1}{3}{u_2}^2 - {u_1}^2\right) \\ -\frac{1}{2}u_1\left(1+\frac{1}{3}{u_1}^2 - {u_2}^2\right) \\ -\frac{1}{2}u_1u_2 \end{pmatrix} . \tag{5.8}$$

We can show the Enneper surface and its conjugate are indeed the same surface by considering a rotation of the domain and a 45° rotation of the image given by:

$$R = \begin{pmatrix} \frac{\sqrt{2}}{2} & -\frac{\sqrt{2}}{2} & 0 \\ \frac{\sqrt{2}}{2} & \frac{\sqrt{2}}{2} & 0 \\ 0 & 0 & 1 \end{pmatrix} . \tag{5.9}$$

Some simple algebra does then indeed confirm (5.6) and (5.8) are the same. Next we shall construct the catenoid.

5.2 The Catenoid

Euler discovered that the catenoid is minimal in 1744. After the plane, it was the first minimal surface to be discovered and these are the only two minimal surfaces which are also surfaces of revolution. It is possible to create a catenoid using soap films. As discussed in the introduction, soap films with given boundaries take the shape of minimal surfaces. To the create the catenoid one can hold two circular boundaries near each other.

The Weierstrass representation for the catenoid is given by:

$$f(z) = -\frac{1}{2}e^{-z} , \qquad g(z) = -e^{z} . \tag{5.10}$$

It is easy to see that both of these functions are holomorphic, and hence this is a valid Weierstrass representation with all of $\mathbb{R}^2$ as the domain. Therefore we can say:

$$\vec{\phi} = \begin{pmatrix} -\frac{1}{4}(e^{-z} - e^{z}) \\ -i\frac{1}{4}(e^{-z} + e^{z}) \\ \frac{1}{2} \end{pmatrix} . \tag{5.11}$$

Throughout the following computation we shall make the assumption that all constants of integration are equal to 0. This is equivalent to defining our surface up to a translation which we are free to do as a translation of a minimal surface does not affect any of its properties.

The Weierstrass representation requires us to integrate this to calculate the surface, and we shall look at this component by component. Due to the fact that all of these functions are holomorphic we can perform the integration and find a primitive which we can then use to define the surface. We begin by integrating ϕ_1:

$$\int \phi_1 \, dz = \int -\frac{1}{4}(e^{-z} - e^{z}) \, dz \tag{5.12}$$
$$= \frac{1}{4}(e^{-z} + e^{z}) + C \,. \tag{5.13}$$

We can discard the C under the above assumption and we shall do so in all further calculations. We must take the real part of this to give an explicit expression for the coordinate function To do this we shall recall Euler's formula $e^{x+iy} = e^{x}(\cos(y) + i\sin(y))$ and find:

$$\sigma_1(u_1, u_2) = \Re\left[\frac{1}{4}(e^{-(u_1+iu_2)} + e^{u_1+iu_2})\right] \tag{5.14}$$
$$= \Re\left[\frac{1}{4}e^{-u_1}(\cos(-u_2) + i\sin(-u_2)) + e^{u_1}(\cos(u_2) + i\sin(u_2))\right] \,. \tag{5.15}$$

Using the fact that $\cos(x)$ is an even function, $\sin(x)$ is an odd function and the identity $\cosh(x) = \frac{1}{2}(e^{x} + e^{-x})$ we can see the above equation is equal to:

$$\sigma_1(u_1, u_2) = \Re\left[\frac{1}{2}\cosh(u_1)\cos(u_2)\right] = \frac{1}{2}\cosh(u_1)\cos(u_2) \,. \tag{5.16}$$

Next, we integrate σ_2 and find:

$$\int \phi_2 \, dz = \int -\frac{i}{4}(e^{-z} + e^{z}) \, dz = \frac{i}{4}(e^{z} - e^{-z}) \,. \tag{5.17}$$

Taking the real part of this then gives:

$$\sigma_2(u_1, u_2) = \Re\left[\frac{i}{4}(e^{u_1+iu_2} - e^{-u_1-iu_2})\right] \tag{5.18}$$
$$= \Re\left[\frac{i}{4}(e^{u_1}(\cos(u_2) + i\sin(u_2)) - e^{-u_1}(\cos(-u_2) + i\sin(-u_2)))\right] \tag{5.19}$$
$$= -\frac{1}{2}\cosh(u_1)\sin(u_2) \,. \tag{5.20}$$

Finally, the integral of ϕ_3 is given by:

$$\int \phi_3 \, dz = \int \frac{1}{2} \, dz = \frac{1}{2}z + C \,. \tag{5.21}$$

Hence it is easy to see that:

$$\sigma_3(u_1, u_2) = \Re[\frac{1}{2}(u_1 + iu_2)] = \frac{1}{2}u_1 \,. \tag{5.22}$$

So we have been able to explicitly integrate the Weierstrass representation for the catenoid, we then arrive at:

$$\vec{\sigma}(u_1, u_2) = \frac{1}{2}\begin{pmatrix} \cosh(u_1)\cos(u_2) \\ -\cosh(u_1)\sin(u_2) \\ u_1 \end{pmatrix} \,. \tag{5.23}$$

We can see by visually inspecting this equation, the result is indeed a surface of revolution, with u_2 parameterising the angle, and paths of constant u_1 giving caternaries. Indeed plotting this we get the following:

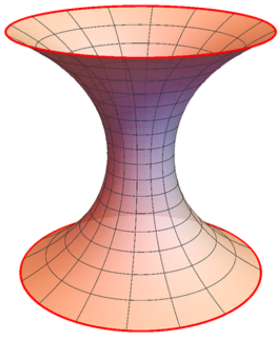

Figure 5: A section of the catenoid plotted for $u_1 \in [-1, 1]$.

We shall now move on to the helicoid.

5.3 The Helicoid

The helicoid was the next minimal surface discovered, a full 30 years after the catenoid. The surface was first described in 1774 by Euler, and was also written about in 1776 by Jean Baptiste Meusnier. Other than the plane, the helicoid is the only ruled minimal surface.

We we will again calculate the exact equation of the helicoid from its Weierstrass representation, which in this case is given by:

$$f(z) = -i\frac{1}{2}e^{-z}, \qquad\qquad g(z) = -e^{z}\,. \tag{5.24}$$

These functions are indeed holomorphic, so once again we are free to take all of $\mathbb{R}^2$ as our domain. It is remarkable how similar this parameterisation is to that of the catenoid, and also how they have such similar properties.

Now when we calculate $\vec{\phi}$ for the catenoid it takes the following form:

$$\vec{\phi} = \begin{pmatrix} -i\frac{1}{4}(e^{-z} - e^{z}) \\ \frac{1}{4}(e^{-z} + e^{z}) \\ \frac{1}{2}i \end{pmatrix}. \tag{5.25}$$

Similarly as before integrating ϕ_1 gives:

$$\int \phi_1 \, dz = -i\frac{1}{4}(e^{-z} - e^{z}) \tag{5.26}$$

$$= i\frac{1}{4}(e^{z} + e^{-z}) + C\,. \tag{5.27}$$

Repeating the process as before we can take the real part, letting $C = 0$. Again we take the real part to calculate the coordinate function.

$$\sigma(u_1, u_2) = \Re[i\frac{1}{4}(e^{u_1}(cos(u_2) + i\sin(u_2)) - e^{-u_1}(\cos(u_2) - i\sin(u_2))]\,. \tag{5.28}$$

After taking the real part we can use the identity $\sinh(x) = \frac{1}{2}(e^x - e^{-x})$ to see this is equal to:

$$\sigma_1(u_1, u_2) = \frac{1}{4}(-e^{u_1}\sin(u_2)) + e^{-u_1}\sin(u_2)) \tag{5.29}$$
$$= -\frac{1}{2}\sinh\sin(u_2)\,. \tag{5.30}$$

Similarly for ϕ_2 we can integrate and take the real part to find:

$$\int \phi_2\; dz = \frac{1}{4}(e^{-z} + e^{z})\; dz \tag{5.31}$$
$$= \frac{1}{4}(e^{z} - e^{-z}) + C \tag{5.32}$$

For the coordinate function we take the real part:

$$\sigma_2(u_1, u_2) = \Re\left[\frac{1}{4}(e^{u_1+iu_2} - e^{-(u_1+iu_2)})\right] \tag{5.33}$$
$$= \Re\left[\frac{1}{4}(e^{u_1}(\cos(u_2) + i\sin(u_2)) - e^{-u_1}(\cos(u_2) - i\sin(u_2)))\right] \tag{5.34}$$
$$= \Re[\left[\frac{1}{4}(e^{u_1}(\cos(u_2) + i\sin(u_2)) - e^{-u_1}(\cos(u_2) - i\sin(u_2)))\right] \tag{5.35}$$
$$= \frac{1}{4}(e^{u_1}\cos(u_2) - e^{-u_1}\cos(u_2)) \tag{5.36}$$
$$= \frac{1}{2}\sinh(u_1)\cos(u_2) \tag{5.37}$$

A similar treatment of ϕ_3 gives:

$$\int \phi_3\; dz = \int \frac{1}{2}i\; dz \tag{5.38}$$
$$= \frac{1}{2}iz + C \tag{5.39}$$

Taking again $C = 0$, it is easy to then see that the final coordinate function is given by:

$$\sigma_3(u_1, u_2) = \Re\left[\frac{1}{2}(iu_1 - u_2)\right] = -\frac{1}{2}u_2\,. \tag{5.40}$$

Hence once we have combined all this we can see the parametric equation for the helicoid is given by:

$$\vec{\sigma}(u_1, u_2) = \frac{1}{2}\begin{pmatrix} -\sinh(u_1)\sin(u_2) \\ \sinh(u_1)\cos(u_2) \\ -u_2 \end{pmatrix}\,. \tag{5.41}$$

Plotting the above equation we indeed find the helicoid:

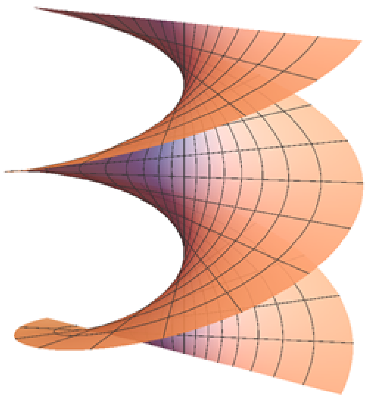

Figure 6: A section of the helicoid which shows both the helices, which are the lines of constant u_2, and the straight lines, which are the lines of constant u_1 contained in the surface.

Tthe catenoid and helicoid equations look very similar, but produce extremely different surfaces with different topology. We shall, however, see how we can unify the catenoid and helicoid into a single associate family.

5.4 The Catenoid–Helicoid Associate Family

In this section we shall explore the how the catenoid and helicoid are in fact two members of an associate family of minimal surfaces. We shall see that the properties of the family allows us to gain insights into the form of each of the surfaces just by looking at properties of the other.

Let us recall from the section on associate families, the definition:

$$\vec{\sigma}_\theta(u_1, u_2) = \Re e^{i\theta} \int_{x_0}^{u_1+iu_2} \begin{pmatrix} \frac{1}{2}f(1-g^2) \\ \frac{i}{2}f(1-g^2) \\ fg \end{pmatrix} dz \tag{5.42}$$

From this we can see that the conjugate pairs of surfaces arise when f is rotated by $90°$ in the complex plane. From this we can see that the catenoid and helicoid do indeed form a conjugate pair as:

$$-\frac{1}{2}e^{-z} \to -i\frac{1}{2}e^{-z}. \tag{5.43}$$

We shall see if we can find an explicit expression for the family, parameterised by θ. We shall start with the integrated expression for the catenoid before we take the real component:

$$\vec{\sigma}_\theta(u_1, u_2) = \Re \left[e^{i\theta} \frac{1}{4} \begin{pmatrix} e^{u_1+iu_2} + e^{-u_1-iu_2} \\ i(e^{u_1+iu_2} - e^{-u_1-iu_2}) \\ 2(u_1+iu_2) \end{pmatrix} \right]. \tag{5.44}$$

This calculation has been omitted as it is very similar to that of the Enneper surface, the catenoid, and the helicoid and it offers no further insight. However, the calculation can be found in full in Appendix A. The resulting equation for the surface is:

$$\vec{\sigma}_\theta(u_1, u_2) = \frac{1}{2}\begin{pmatrix} \cosh(u_1)\cos(u_2)\cos(\theta) - \sinh(u_1)\sin(u_2)\sin(\theta) \\ -\cosh(u_1)\sin(u_2)\cos(\theta) + \sinh(u_1)\cos(u_2)\sin(\theta) \\ u_1\cos(\theta) - u_2\sin(\theta) \end{pmatrix}. \tag{5.45}$$

We can see from this equation that each point on the surface moves in an ellipse as θ varies. We now plot this equation for multiple values of θ to visualise the transformation taking place.

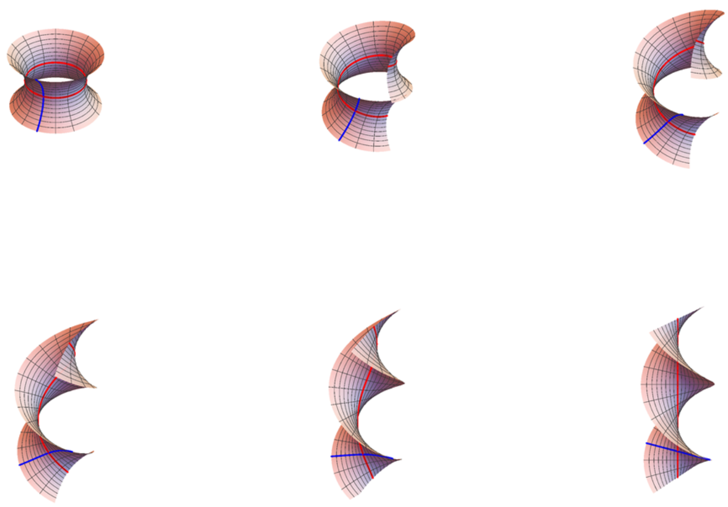

Figure 7: This shows the catenoid helicoid–associate family for values $\theta \in \{0, \frac{\pi}{10}, \frac{\pi}{5}, \frac{3\pi}{10}, \frac{2\pi}{5}, \frac{\pi}{2}\}$. The two different types of planar geodesics are also highlighted, with the curve obtained by intersecting the catenoid with the $z = 0$ plane highlighted in red, which then maps to the z axis. A path of constant u_2 is shown in blue.

Using figure 7, we can also see how paths in the catenoid correspond to paths in the helicoid. For example, paths of constant u_2, which are catenaries at $\theta = 0$ map to straight lines in the helicoid. This result is consistent with Theorem 5, however it is still remarkable as the curves which foliate the catenoid are the straight lines which foliate the helicoid. The catenaries foliate the catenoid by angle, so a catenary at angle t maps to a line in the helicoid rotated by 90° i.e. $t + \frac{\pi}{2}$.

Another interesting path is the circle in the catenoid generated when $u_1 = 0$, which maps to the z-axis contained helicoid, shown in red in figure 7.

So we do indeed have the paths in the surface generated by planes of symmetry mapping to straight lines in the conjugate surface. Notice the helicoid has no planes of symmetry, and hence from this we can see that the catenoid has no straight lines contained in it. However it is interesting to see that the circles obtained by keeping u_1 constant in the catenoid map to the helices which give the helicoid its name.

All surfaces in this family are isometric, so locally the structure of the surface does not change, not only that but each surface is parameterised isothermally, hence angles between paths are always preserved during the entire transformation. It is also clear that the transformation between surfaces in the family is smooth with respect to derivatives of θ because $e^{i\theta}$ is a smooth function, so all derivatives exist. So locally, anything embedded in the surface is not aware that the transformation is taking place. However the global topology of the surface changes. The helicoid is simply connected however the catenoid is not, the circle contained in the $z = 0$ plane and the catenoid is a closed path, however in the helicoid this path is infinitely long. Using this fact it is also obvious that the catenoid is covered multiple times for values of $u_2 > 2\pi$, sections of the helicoid that differ by a change in u_2 of 2π are indeed identical, so the rotational symmetry of the catenoid has in some sense generated the translational symmetry of the helicoid.

This shows the usefulness in the Weierstrass representation, it has been able to unify the first two non-planar minimal surfaces into one continuous isometric family. It is not at all obvious that two surfaces as different as the catenoid and helicoid would have the same structure, however this is immediately obvious once they have been presented using the Weierstrass representation.

Next we shall look at the Costa surface.

6 The Costa Surface

In 1982 Costa showed in his PhD thesis [5] that there exists a surface of genus one and three embedded ends. Although we shall not give a precise definition, here an end is a way of approaching infinity from inside the surface. However he did not show that the entre surface is embedded, only that it is embedded outside of a large enough region. Three years later, in 1985, however David Hoffman and William Meeks published a paper [11] proving that all of the surface is embedded in $\mathbb{R}^3$, this was a great breakthrough in the study of minimal surfaces as it took over 200 years of study to find a complete embedded minimal surface of finite genus. The Costa surface was also the stepping stone needed to generalise complete embeddedness to any finite genus [15].

In this section we shall look at the construction, via the Weierstrass representation, and properties of the Costa surface.

The surface is parameterised using elliptic functions, i.e. meromorphic functions which are periodic in 2 directions. Elliptic functions have been studied for a long time, so much is known about them. There are two main kinds of elliptic functions, Jacobi and Weierstrass, but the Costa surface is defined just using the Weierstrass P function, denoted $\wp(z)$, which we shall define and study in the next section.

6.1 The Weierstrass P function

The Weierstrass P function is elliptic, that is to say it is a complex function which is periodic in two directions. The Weierstrass P function is defined generally on a lattice in $\mathbb{C}$, denoted $\Lambda = \{m\omega_1 + n\omega_2 : m, n \in \mathbb{Z}\}$, where ω_1 and ω_2 are linearly independent complex numbers,which we call the periods of the function. $\wp(z; \omega_1, \omega_2)$ is given by the following expression:

$$\wp(z) := \frac{1}{z^2} + \sum_{\omega \in \Lambda \setminus \{0\}} \left(\frac{1}{(z-\omega)^2} - \frac{1}{\omega^2} \right) . \tag{6.1}$$

It is easy to see that there is a pole of order 2 at $z = 0$, so we also get poles of order 2 at each point in the lattice Λ.

Theorem 6 (The P function is doubly periodic)**.** The Weierstrass P function is uniquely defined by its value on a fundamental domain given by the generators of the lattice. Then, $\wp(z) = \wp(z+\omega)$ for all $\omega \in \Lambda$.

Proof. To show this, let us consider any z in the fundamental domain and consider $z \mapsto z + \omega_0$ for any ω_0 in $\Lambda \setminus \{0\}$ then we get

$$\wp(z+\omega_0) = \frac{1}{(z+\omega_0)^2} + \sum_{\omega \in \Lambda \setminus \{0\}} \left(\frac{1}{(z+\omega_0-\omega)^2} - \frac{1}{\omega^2} \right) \tag{6.2}$$

$$= \frac{1}{(z+\omega_0)^2} + \sum_{\omega \in \Lambda \setminus \{0\}} \left(\frac{1}{(z+\omega_0-\omega)^2} \right) - \sum_{\omega \in \Lambda \setminus \{0\}} \left(\frac{1}{\omega^2} \right) . \tag{6.3}$$

We can remove the $\frac{1}{(z+\omega_0-\omega_0)^2}$ from the sum by removing ω_0 from the lattice, we then add this term back in explicitly. In the second term we shall just sum over ω, and by this we shall always mean the original lattice with the point 0 removed:

$$= \frac{1}{(z+\omega_0)^2} + \frac{1}{(z+\omega_0-\omega_0)^2} + \sum_{\omega \in \Lambda \setminus \{0,\omega_0\}} \left(\frac{1}{(z+\omega_0-\omega)^2} \right) - \sum_{\omega} \left(\frac{1}{\omega^2} \right) \tag{6.4}$$

$$= \frac{1}{z^2} + \frac{1}{(z+\omega_0)^2} + \sum_{\omega \in \Lambda \setminus \{0,\omega_0\}} \left(\frac{1}{(z+\omega_0-\omega)^2} \right) - \sum_{\omega} \left(\frac{1}{\omega^2} \right) . \tag{6.5}$$

Incorporating the $\frac{1}{(z+\omega_0)^2}$ into the sum over the lattice can be done by adding the point 0 back into the sum, like so:

$$\wp(z+\omega_0) = \frac{1}{z^2} + \sum_{\omega \in \Lambda \setminus \{\omega_0\}} \left(\frac{1}{(z+\omega_0-\omega)^2} \right) - \sum_{\omega} \left(\frac{1}{\omega^2} \right) \tag{6.6}$$

$$= \frac{1}{z^2} + \sum_{\omega \in \Lambda \setminus \{\omega_0\}} \left(\frac{1}{(z-(\omega-\omega_0))^2} \right) - \sum_{\omega} \left(\frac{1}{\omega^2} \right) . \tag{6.7}$$

Now we can consider the translation where all $\omega - \omega_0 \mapsto \omega$, as we have removed the point ω_0 from our lattice. Once we have done this translation, the only point missing will be 0:

$$\wp(z+\omega_0) = \frac{1}{z^2} + \sum_{\omega \in \Lambda \setminus \{0\}} \left(\frac{1}{(z-\omega)^2} \right) - \sum_{\omega} \left(\frac{1}{\omega^2} \right) \tag{6.8}$$

$$= \frac{1}{z^2} + \sum_{\omega \in \Lambda \setminus \{0\}} \left(\frac{1}{(z-\omega)^2} - \frac{1}{\omega^2} \right) \tag{6.9}$$

$$= \wp(z) .$$

□

The lattice used to create the Costa surface is constructed using the generators 1 and i, which are of course linearly independent. From now on we shall assume this lattice when we use the Weierstrass P function. Let us study some properties of this specific P function. Firstly it is also worth noting that this function has a zero of order two at the point $\frac{1}{2} + \frac{i}{2}$ which is of order 2.

The derivative of the P function is given by:

$$\wp'(z) = \frac{-2}{z^3} - \sum_{\omega \in \Lambda \setminus \{0\}} \left(\frac{2}{(z-\omega)^3} + \frac{1}{\omega^2} \right) . \tag{6.10}$$

We can see this function is again defined by its values on a fundamental domain, which is what we expected.

A classical result in the theory of elliptic functions is that they obey the following differential equation,

$$(\wp'(z))^2 = 4(\wp(z) - e_1)(\wp(z) - e_2)(\wp(z) - e_3), \tag{6.11}$$

where e_i are the values at the critical points of $\wp(z)$. We have three critical points, which we shall label $\omega_1 = \frac{i}{2}$, $\omega_2 = \frac{1}{2}$ and $\omega_3 = \frac{1}{2} + \frac{i}{2}$. And computing the value $\wp(\omega_i)$ we get, $e_1 = -e_2 = 6.875\ldots$ and $e_3 = 0$. Hence we can say:

$$(\wp')^2 = 4\wp(\wp - e_1)(\wp + e_1) . \tag{6.12}$$

For the rest of the paper we shall concern ourselves with Hoffman and Meeks' paper's [11] construction of the symmetries of the Costa surface. This paper also goes on to show that the surface is indeed embedded, however we shall not show this here.

6.2 Showing the Symmetries of $\wp$

Firstly recall some theorems required for the following construction.

Theorem 7 (Schwarz Reflection Principle)**.** Taken from [13] Suppose we have a complex function, f, which is holomorphic on some subdomain of $\mathbb{C}$ with at least one straight edge, and let the values of f alone this straight edge be mapped to a straight line in $\mathbb{C}$. If we then take the reflection of the domain and image in this straight line, then the result is a holomorphic function. including along the line of reflection.

Theorem 8 (Holomorphic Functions with Identical Poles and Zeros)**.** Given two meromorphic functions, f and g, such that f has a pole of order m at $z \iff g$ has a pole of order m at z, and the same for each zero for all of $\bar{\mathbb{C}}$, then the two functions are related via $f(z) = cg(z)$, where c is some constant, $c \in \mathbb{C}$.

The next steps in the construction are the following:

1. We start by constructing an elliptic function ϕ.

2. We see that f is elliptic and has the same poles and zeros as g.

3. From this we deduce $f(z) = k\wp(z)$ and $f(\omega_1) = \wp(\omega_1)$ which implies $f \equiv \wp$.

We shall call our elliptic function ϕ. Using small parts of the desired domain and theorem 7, we shall firstly consider just a small domain from which we will construct a meromorphic function on all of $\bar{\mathbb{C}}$. Our target fundamental domain is the unit square in the complex plane. We shall split this domain up into 8 regions which shall be used in the construction of ϕ in the following manner:

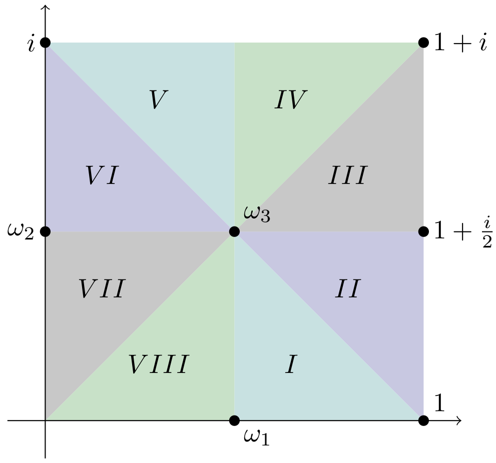

Figure 8: The regions of the domain which shall be used to construct the Weierstrass P function.

The Weierstrass P function when plotted for the region I in figure 8 takes on all values in the positive quadrant of the complex plain, including infinity. We shall use this triangle as a fundamental unit from which we shall construct $\wp$.

We define a transformation of I, which we shall call $f(z)$, $z \in I$, which maps the vertices of the triangle I in figure 8, such that $f(\omega_3) = 0$, $f(\omega_1) = e_1$ and $f(1) = \infty$.

We can construct this transformation ensuring that it is meromorphic on all of I, and indeed holomorphic on $I \setminus \{1\}$. We do this by using the Riemann mapping theorem to construct a map, $f_D : I \to D(0,1)$, where $D(0,1)$ is the unit disk centred at the origin. We also note that this mapping is, by the Riemann mapping theorem, both bijective and holomorphic. We can then construct another map $f_Q : D(0,1) \to Q$, where Q is the positive quadrant. We note that the boundary of the positive quadrant is a Jordan curve on the Riemann sphere, and hence we can use Carathéodory's theorem as stated in [14] to continuously extend this map onto the closure of I, denoted $\bar{I}$. So the composition of these functions, $f_Q \circ f_D = f$ is a holomorphic function which maps $\bar{I}$ to the positive quadrant, such that the boundary of I maps to either the positive real or positive imaginary axis in a nice way.

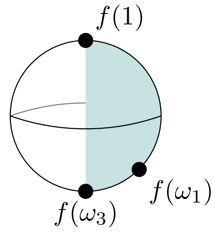

Figure 9: This figure shows the image of the transformation of I stereographically projected onto the Riemann sphere. We see the transformation maps to the whole of the positive quadrant, and hence fills one quarter of the Riemann sphere. We can see from this diagram that the line connecting ω_3 to 1 in the domain maps to the positive real axis, and the line connecting ω_1 to ω_3 maps to a portion of the real axis.

We can see from the figure 9 that the line $\overrightarrow{\omega_3, 1}$, the hypotenuse of region I, maps to the real axis and hence $f(z)$ takes purely real values along this line. We can also see that the line corresponding to $\overrightarrow{\omega_3, 1}$ maps to the imaginary axis and thus $f(z)$ is pure imaginary.

We can then use Theorem 7 to extend our definition. We shall reflect our domain in the line $\overrightarrow{\omega_1, \omega_3}$, which is given by $\mu(z) = \omega_1 - i\overline{(z - \omega_1)}$ and extend ϕ by reflecting f in the real axis, which is given by complex conjugation, so we can extend the definition of ϕ thusly

$$\phi(z) = \begin{cases} f(z) & z \in I \\ \overline{f(\mu(z))} & z \in II \end{cases} . \tag{6.13}$$

Now our domain has been extended to the square with vertices $\frac{1}{2}$, $\frac{1}{2} + \frac{i}{2}$, $1 + \frac{i}{2}$ and 1, we also know that $\phi(z)$ is imaginary along the top of the square domain formed by $I \cup II$, namely the line $\overrightarrow{\frac{1}{2} + \frac{i}{2}, 1 + \frac{i}{2}}$ as this corresponds to the line $\overrightarrow{\omega_1, \omega_3}$. Hence we can reflect the entire square in this line to extend the domain. The reflection in this line is given by $\beta(z) = \omega_3 + \overline{(z - \omega_3)}$ which maps $I \cup II$ into $III \cup IV$. As the line of reflection in the domain corresponds to the imaginary axis in the image, we have to reflect f in the imaginary axis in order to extend ϕ, which is given by $-\overline{f}$, and hence we can give an updated version of ϕ:

$$\phi(z) = \begin{cases} f(z) & z \in I \\ \overline{f(\mu(z))} & z \in II \\ -\overline{f(\beta(z))} & z \in III \cup IV \end{cases} . \tag{6.14}$$

We can now extend ϕ to cover the entirety of the unit square by reflecting in the line $\overrightarrow{\frac{1}{2}, \frac{1}{2} + i}$. The image of this line with the current definition of ϕ is the imaginary axis, thus we do one last reflection along this axis. The reflection in the domain is given by $\lambda(z) = \frac{1}{2} - \overline{z - \omega_3}$, and reflecting

ϕ in the real axis, we have the entire construction of ϕ on the unit square.

$$\phi(z) = \begin{cases} f(z) & z \in I \\ \overline{f(\mu(z))} & z \in II \\ -\overline{f(\beta(z))} & z \in III \cup IV \\ \overline{f(\lambda(z))} & z \in V \cup VI \cup VII \cup VIII \end{cases} . \tag{6.15}$$

We can then define ϕ over all of $\mathbb{C}$ simply by extending it periodically, with periods 1 and i. We note that the region $IV \cup V$ is a reflection of $I \cup VIII$. Also $II \cup III$ is a reflection of $VI \cup VII$. Therefore, when the function is tiled the result is indeed a meromorphic function, even at the boundaries of each fundamental domain. We now have an elliptic function defined over all of $\mathbb{C}$, which has one pole at the point 0, hence also on each lattice point, and one zero at $\frac{1}{2} + \frac{i}{2}$.

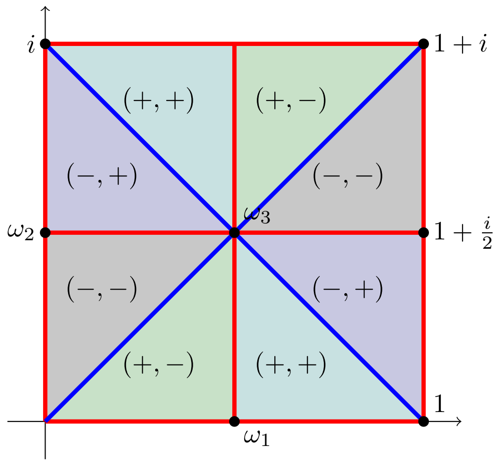

Figure 10: Here we have a domain with the signs of the real and imaginary parts of the image of $\wp(z)$ given in brackets, which give the signs of the real and imaginary parts respectively. It also shows the lines along which the real part is zero, shown in blue, and the lines where the imaginary part is zero, shown in red. We can see that the zero lines cross at ω_3 as the value of the function is identically zero at this point.

To see the order of these poles and zeros we shall look at a path around ω_3 in our domain. First we can see from figure 10 that region I maps into the upper left quadrant. II maps into upper right III into bottom left and IV into bottom right, and so on. So our image looks somewhat like:

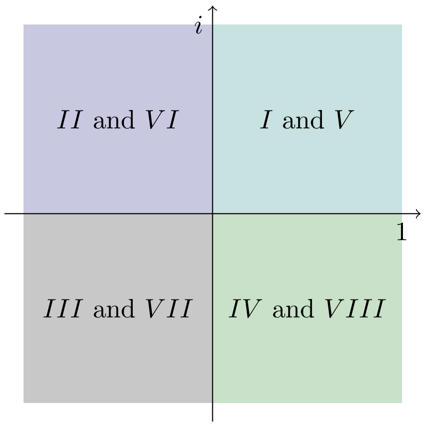

Figure 11: Here we have a diagram of where the different regions of the domain get mapped to in the complex plane. Note that these regions extend all the way to infinity.

From figure 10 we can see that a closed loop around zero in the domain travels through each region once. However in figure 11 we see that the portion of the loop contained in $I \cup II \cup III \cup IV$ makes one full loop around 0 in the domain. Similarly for the section of the curve contained in $V \cup VI \cup VII \cup VIII$ we get a second loop around zero in the domain, and hence $f(\omega_3)$ is a zero with multiplicity 2.

Now, by construction, we have an elliptic function with poles of order 2 at the exact locations $\wp(z)$ has poles of order 2 and zeros of order at exactly where $\wp(z)$ has zeros of order 2, and hence by Theorem 8 the two functions are the same up to a multiplicative constant. However, we also have that $\phi(\omega_1) = \wp(\omega_1) = e_1$, again by construction, so in fact our two functions are identical.

From this we can see that the Weierstrass P function is in fact highly symmetric. We can generate these symmetries by looking at D_8, the dihedral symmetry group of the square. Let us take $\beta(\omega_3 + z) = \omega_3 + \overline{z}$, a reflection in the line $\overrightarrow{\frac{i}{2}, 1 + \frac{i}{2}}$ and $\rho^k(\omega_3 + z) = \omega_3 + i^k z$ which is a rotation with angle $\frac{k\pi}{2}$ around the point ω_3. We can then categorise how these symmetries affect $\wp(z)$:

$$\wp \circ \beta = \overline{\wp}\ , \tag{6.16}$$

$$\wp \circ \rho^k = (-1)^k \wp \tag{6.17}$$

where ρ^k signifies repeated function composition.

From this we can also see that $\wp(\omega_3 + z) = \wp(\omega_3 - z)$, which arises from the case when $k = 2$ in equation (6.17).

6.3 The Weierstrass Representation for the Costa Surface

In this section we shall tie the Weierstrass P function to the construction of the Costa surface and we shall use the properties we have derived to show properties of the Costa surface.

The actual Weierstrass data for the Costa surface is as follows:

$$f(z) = \wp(z)\,, \qquad\qquad g = \frac{2\sqrt{2\pi}\wp(\frac{1}{2})}{\wp'(z)}\,. \tag{6.18}$$

In order to save on writing let $a := 2\sqrt{2\pi}\wp(\frac{1}{2})$.

Due to the doubly periodic nature of both f and g we can study what the surface looks like just by looking at this fundamental domain. Not only is our domain a square, but we can also associate opposite sides with each other, and hence we obtain a torus, T^2. However we must also remove the points of the torus for which the ϕ_k functions are not holomorphic.

The easiest pole to spot is the one which occurs at $z = 0$ which is a pole of order 2 for f, hence neither ϕ_1 nor ϕ_2 is holomorphic at this point therefore we shall remove it from our domain.

$\wp'(z)$ also has a zero at both the points $z = \frac{1}{2}$ and $z = \frac{i}{2}$, generating poles of g which correspond to non-zero values in f. These points must also be removed from our domain.

We can also see that $\wp'(z)$ has a zero of order 1 at the point $z = \frac{1}{2} + \frac{i}{2}$ meaning g has a pole of order 1. However, f also has a zero at this point, but of order 2, and hence all ϕ_k are holomorphic at this point.

And hence we can say the domain for the Weierstrass representation is given by a punctured torus, namely, $T^2 \setminus \{0, \frac{1}{2}, \frac{i}{2}\}$.

The fact that there are three punctures on the torus corresponding to poles implies that the surface has three ends. As we take points in the domain closer and closer to the poles the coordinate functions tend to infinity. However the pole at $f(0)$ corresponds to a zero of order 3 at $g(0)$, and hence the $\vec{\sigma}_3$ coordinate tends to a constant. We call this a planar end of the surface, because outside of a large enough set around the origin the surface looks like a plane.

We have shown that as we head towards the poles in the domain, the surface tends to infinity, and hence the surface fulfils Theorem 10.

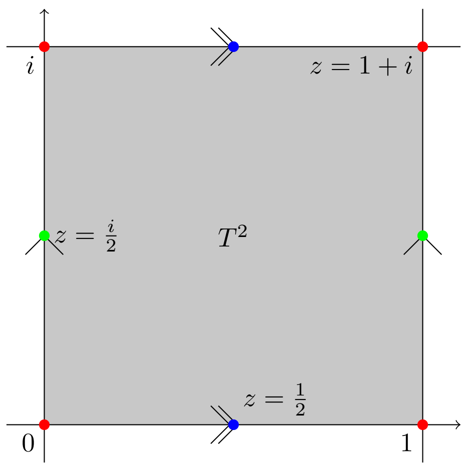

Figure 12: The unit square with sides associated making it topologically equivalent to the tourus. Poles are also marked as circles.

We also want to look at symmetries of the Weierstrass P function as from there we can reconstruct symmetries of the surface.

So computing ϕ for the given Weierstrass representation, we get:

$$\vec{\phi} = \begin{pmatrix} \frac{1}{2}\left(\wp - a^2\frac{\wp}{\wp'^2}\right) \\ \frac{i}{2}\left(\wp + a^2\frac{\wp}{\wp'^2}\right) \\ a\frac{\wp}{\wp'} \end{pmatrix}. \tag{6.19}$$

However by equation (6.12) we can see that $\frac{\wp}{\wp'^2} = \frac{1}{(\wp+e_1)(\wp-e_1)}$, which is easier to work with, and hence we can say:

$$\vec{\phi} = \begin{pmatrix} \frac{1}{2}\left(\wp - \frac{a^2}{4(\wp+e_1)(\wp-e_1)}\right) \\ \frac{i}{2}\left(\wp + \frac{a^2}{4(\wp+e_1)(\wp-e_1)}\right) \\ a\frac{\wp'}{4(\wp+e_1)(\wp-e_1)} \end{pmatrix}. \tag{6.20}$$

Let us firstly look at $\sigma_3(u_1,u_2)$ for the Costa surface, which we obtain by taking the real part of the integral $\sigma_3(u_1,u_2) = \Re\left[\int_{z_0}^{u_1+iu_2} a\frac{\wp'}{4(\wp+e_1)(\wp-e_1)}\, dz\right]$. We shall choose $z_0 = \omega_3$ as $\wp(\omega_3) = 0$ and we can use partial fractions to show:

$$\frac{a\wp'}{4(\wp+e_1)(\wp-e_1)} = \frac{a\wp'}{8e(\wp-e_1)} - \frac{a\wp'}{8e(\wp+e_1)}. \tag{6.21}$$

And from this we can integrate explicitly toget:

$$\int_{\omega_3}^{z} \frac{a\wp'(\xi)}{8e(\wp(\xi)-e_1)} - \frac{a\wp'(\xi)}{8e(\wp(\xi)+e_1)}\, d\xi = \left[\frac{a}{8e_1}\ln\left(\wp(z)-e_1\right) - \frac{a}{8e_1}\ln\left(\wp(z)+e_1\right)\right]_{\omega_3}^{z} \tag{6.22}$$

$$= \frac{a}{8e_1}\ln\left(\frac{\wp(z)-e_1}{\wp(z)+e_1}\right) - \frac{a}{8e_1}\ln\left(\frac{\wp(\omega_3)-e_1}{\wp(\omega_3)+e_1}\right) \tag{6.23}$$

$$= \frac{a}{8e_1}\ln\left(\frac{\wp(z)-e_1}{\wp(z)+e_1}\right) - \frac{a\pi i}{8e_1}. \tag{6.24}$$

When we take the real part we find:

$$\sigma_3(u_1,u_2) = \Re\left[\frac{a}{8e_1}\ln\left(\frac{\wp(u_1+iu_2)-e_1}{\wp(u_1+iu_2)+e_1}\right) - \frac{a\pi i}{8e_1}\right] = \frac{a}{8e_1}\ln\left|\frac{\wp(u_1+iu_2)-e_1}{\wp(u_1+iu_2)+e_1}\right|. \tag{6.25}$$

From this we can see that if the distance in the complex plane from $\wp(u+iu_2)$ to both e_1 and $-e_1$ determines the sign of σ_3, if this value is closer to $-e_1$ then $\left|\frac{\wp(u_1+iu_2)-e_1}{\wp(u_1+iu_2)+e_1}\right| < 1$ and hence σ_3 at this point is negative, when the value is closer to e_1, we then get σ_3 is positive. This only depends on the real value of $\wp(u+iu_2)$: if it is positive then σ_3 is negative and conversely, if $\wp(u_1+iu_2)$ is negative then σ_3 is positive. σ_3 is only zero when $\wp(u+iu_2)$ lies on the imaginary axis. As shown in figure 10, the diagonal lines (shown in blue in the figure), split the domain into 4 regions. $I \cup VIII$ and $IV \cup V$ have positive real parts, and $II \cup III$ and $VI \cup VII$ have negative real parts.

6.3.1 Boundaries of III

In this section we shall look at the image of the boundary of III.

We shall start by looking at where the diagonal line $\overrightarrow{\omega_3, 1+i}$ maps to in our surface. To do this we shall note that $\wp(z)$ is purely imaginary along this line. We shall parameterise the positive diagonal starting at ω_3 as $z = \frac{1}{2}t + \frac{i}{2}t$. We can then say $\wp(\omega_3 + t + it) = -i\alpha(t)$, where $\alpha : \mathbb{R} \to \mathbb{R}$. Also, as we have shown by the construction of the Weierstrass P function via reflections we know the value of $\alpha(t)$ increases monotonically on the line $t \in [0, \frac{1}{2}]$, with $\alpha(0) = 0$ and $\alpha(\frac{1}{2}) = \infty$. Note with this change of variables we find $dz = (1+i)\ dt$.

We can now use $\alpha(t)$ instead of $\wp(z)$ along the diagonals:

$$\sigma_1\left(\frac{1}{2}+t, \frac{1}{2}+t\right) = \Re\left[\int_{\omega_0}^{t+it} \phi_1(z)\ dz\right] \tag{6.26}$$

$$= \Re\left[\int_0^t \frac{1}{2}\left(-i\alpha(t') - \frac{a^2}{4(-i\alpha(t')+e_1)(-i\alpha(t')-e_1)}\right)\ (1+i)dt'\right] \tag{6.27}$$

$$= \Re\left[\int_0^t \frac{1}{2}\left(-i\alpha(t') + \frac{a^2}{4(\alpha(t')^2+e_1{}^2)}\right)\ (1+i)dt'\right] \tag{6.28}$$

$$= \int_0^t \frac{1}{2}\left(\alpha(t') + \frac{a^2}{4(\alpha(t')^2+e_1{}^2)}\right)\ dt'\,. \tag{6.29}$$

Now similarly for σ_2:

$$\sigma_2\left(\frac{1}{2}+t, \frac{1}{2}+t\right) = \Re\left[\int_{\omega_0}^{t+it} \phi_2(z)\ dz\right] \tag{6.30}$$

$$= \Re\left[\int_0^t \frac{i}{2}\left(-i\alpha(t') - \frac{a^2}{4(\alpha(t')^2-e_1{}^2)}\right)\ (1+i)dt'\right] \tag{6.31}$$

$$= \int_0^t \frac{1}{2}\left(\alpha(t') - \frac{a^2}{4(\alpha(t')^2-e_1{}^2)}\right)\ dt' \tag{6.32}$$

$$= \sigma_1\left(\frac{1}{2}+t, \frac{1}{2}+t\right)\,. \tag{6.33}$$

So we see that $\sigma_1\left(\frac{1}{2}+t, \frac{1}{2}+t\right) = \sigma_2\left(\frac{1}{2}+t, \frac{1}{2}+t\right)$, $\sigma_3\left(\frac{1}{2}+t, \frac{1}{2}+t\right) = 0$, $t \in [0, \frac{1}{2}]$. This parameterises the straight line $x = y,\ z = 0$ for $x > 0$. We know $\alpha(t)$ increases monotonically, and hence the integral, $\int \alpha(t)$ also increases monotonically, so we can say that $\vec{\sigma}\left(\frac{1}{2}+t, \frac{1}{2}+t\right)$ is injective for $t \in [0, \frac{1}{2}]$.

Now we shall look at the line $\overrightarrow{\omega_3, \omega_3 + \frac{1}{2}}$. We can see, by our construction that $\wp(\frac{1}{2}+t+\frac{i}{2})$ takes on real values for $t \in [0, \frac{1}{2}]$. Once again we can let $\wp(\frac{1}{2}+t+\frac{i}{2}) = -\gamma(t)$ for some monotonically increasing function $\gamma : \mathbb{R} \to \mathbb{R}$. We can also note that $\gamma(0) = 0$ and $\gamma(1) = e_1$. We can now see that the second coordinate is then given by:

$$\sigma_2\left(\frac{1}{2}+t, \frac{1}{2}\right) = \Re\int_{\omega_3}^{\omega_3+t} \frac{i}{2}\left(\wp(z) + \frac{a^2}{\wp(z)^2-e_1{}^2}\right)\ dz \tag{6.34}$$

$$= \Re\int_0^t \frac{i}{2}\left(-\gamma(t') + \frac{a^2}{\gamma(t')^2-e_1{}^2}\right)\ dt' \tag{6.35}$$

$$= 0\,. \tag{6.36}$$

So this boundary is contained in the x, z plane. For σ_1, we get:

$$\sigma_1\left(\frac{1}{2}+t, \frac{1}{2}\right) = \Re\int_{\omega_3}^{\omega_3+t} \frac{1}{2}\left(\wp(z) - \frac{a^2}{\wp(z)^2-e_1{}^2}\right)\ dz \tag{6.37}$$

$$= \int_0^t \frac{1}{2}\left(-\gamma + \frac{a^2}{e_1{}^2-\gamma(t')^2}\right)\ dt'\,. \tag{6.38}$$

Since $\gamma(t) \to e_1$ then ${e_1}^2 - \gamma(t)^2 \to 0$ and hence our coordinate function tends to infinity.

$$\sigma_3\left(\frac{1}{2}+t, \frac{1}{2}\right) = \frac{a}{8e_1} \ln\left|\frac{-\gamma(t)-e_1}{-\gamma(t)+e_1}\right| = \frac{a}{8e_1} \ln\left|\frac{\gamma(t)+e_1}{\gamma(t)-e_1}\right| . \tag{6.39}$$

So we can see that $\sigma_3(\frac{1}{2}+t, \frac{1}{2}) = 0 \iff t = 0$, and also, σ_3 increases towards infinity as $t \to \frac{1}{2}$.

Now the final boundary we want to look at is the line $\overrightarrow{1+\frac{i}{2}, 1+i}$. We want to show it is contained y,z-plane. Again $\wp(z)$ is pure real along this line, so we shall say $\wp(1+\frac{i}{2}+it) = -\eta(t)$, again with $\eta : \mathbb{R} \to \mathbb{R}$ and $\eta(0) = e_1$, $\eta(\frac{1}{2}) = \infty$.

$$\sigma_1\left(1, \frac{1}{2}+t\right) = \Re\left[\int_{\omega_0}^{1+\frac{i}{2}+it} \phi_1(z)\, dz\right] \tag{6.40}$$

$$= \Re\left[\int_1^{\frac{1}{2}} \phi_1(z)\, idt\right] \tag{6.41}$$

$$= \Re\left[i\int_0^t \frac{1}{2}\left(-\eta(t') + \frac{a^2}{\eta(t')^2 - {e_1}^2}\right) dt'\right] . \tag{6.42}$$

This integral is clearly real, and as we are multiplying by i and taking the real part it is trivial to see that:

$$\sigma_1\left(1, \frac{1}{2}+t\right) = 0 \tag{6.43}$$

which shows that the image of this boundary is indeed contained in the (y,z) plane.

Now computing $\sigma_3(1, \frac{1}{2}+t)$, we can use η along this path, to get the following expression:

$$\sigma_3\left(\frac{1}{2}+t, \frac{1}{2}\right) = \frac{a}{8e_1} \ln\left|\frac{-\eta(t)-e_1}{-\eta(t)+e_1}\right| = \frac{a}{8e_1} \ln\left|\frac{\eta(t)+e_1}{\eta(t)-e_1}\right| . \tag{6.44}$$

We note that $\eta(0) = e_1$, and hence σ_3 tends towards infinity as t tends to 0. As t tends to infinity so does $\eta(t)$, and hence $\frac{\eta(t)+e_1}{\eta(t)-e_1} \to 1$, so σ_3 tends to 0.

When we graph the boundaries of region three we get the following:

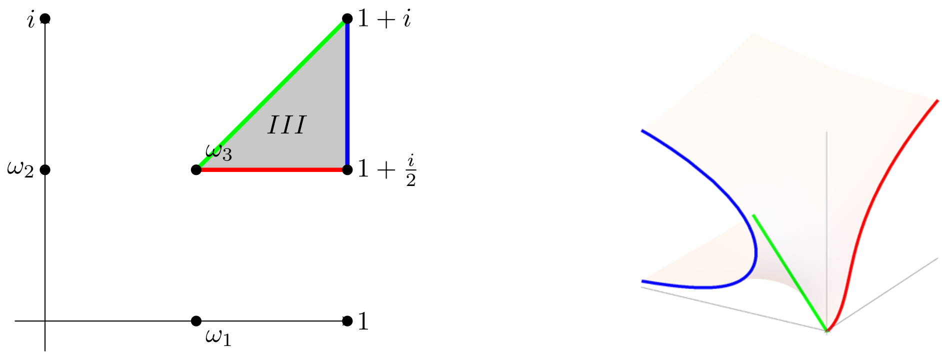

Figure 13: A plot of a section of the Costa surface showing where the boundaries of the region III are mapped to, with the colour of the path in the domain (left) corresponding to colour of the path in the image (right). We can see from this plot that region III maps into the positive quadrant of $\mathbb{R}^3$.

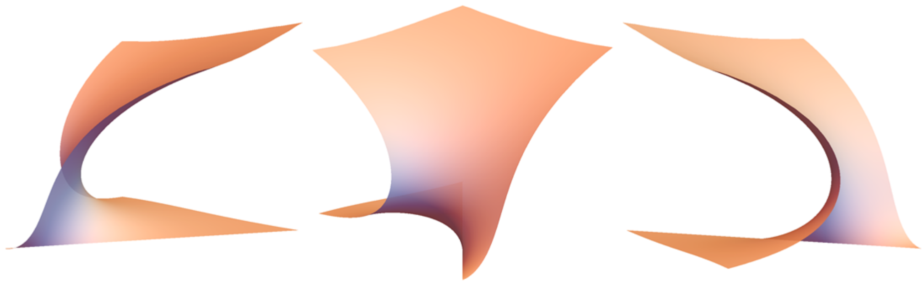

Figure 14: The fundamental unit of the Costa surface plotted from three different viewpoints.

6.3.2 Symmetries of the Costa Surface

In this section we shall look at how the symmetries of the function $\wp$ relate to symmetries of the Costa surface. Recall equations (6.16) and (6.17)

$$\wp \circ \beta = \overline{\wp}\,, \tag{6.45}$$

$$\wp \circ \rho^k = (-1)^k \wp \tag{6.46}$$

we shall use these symmeteries of $\wp$ to derive the symmetries of the Costa surface.

Let us first look at the symmetry generated by (6.17), we shall look at each coordinate function individually, starting with σ_1:

$$\sigma_1(\omega_3 + z) = \Re \int_{\omega_3}^{\omega_3+z} \frac{1}{2}\left(\wp(\xi) - \frac{a^2}{4\wp(\xi)^2 - {e_1}^2}\right)\, d\xi\,. \tag{6.47}$$

We now want to change the integration variable $z \to -i\xi$, which implies, $d\xi \to -id\xi$. We also need to check how the limits of the integral change $\omega_3 \to i\omega_3 = -\frac{1}{2} + \frac{i}{2} = \omega_3 - 1$ and similarly $\omega_3 + z \to \omega_3 + iz - 1$, but the -1 corresponds to a translation of exactly one period of our elliptic function, hence the integral does not change when we translate back to our fundamental domain:

$$\sigma_1(\omega_3 + z) = \Re \int_{\omega_3}^{\omega_3+iz} \frac{1}{2}\left(\wp(-i\xi) - \frac{a^2}{4\wp(-i\xi)^2 - {e_1}^2}\right)\, (-i)d\xi\,. \tag{6.48}$$

Now using the symmetry derived for ρ, we get:

$$\sigma_1(\omega_3 + z) = \Re \int_{\omega_3}^{\omega_3+iz} -\frac{1}{2}\left(\wp(\xi) + \frac{a^2}{4\wp(\xi)^2 - {e_1}^2}\right)\, (-i)d\xi\,. \tag{6.49}$$

We can see that this in fact gives us a multiple of ϕ_2:

$$\sigma_1(\omega_3 + z) = \Re \int_{\omega_3}^{\omega_3+iz} i\phi_2(\xi)\,(-i)d\xi \tag{6.50}$$

$$= \int_{\omega_3}^{\omega_3+iz} -\phi_2(\xi)\, d\xi \tag{6.51}$$

$$= -\sigma_2(\rho(\omega_3 + z))\,. \tag{6.52}$$

And hence we can see how ρ acts on the second coordinate function, $\sigma_2(\rho(\omega_3 + z)) = -\sigma_1(\omega_3 + z)$

Continuing with a similar treatment for σ_2, we find:

$$\sigma_2(\omega_3 + z) = \Re \int_{\omega_3}^{\omega_3+z} \frac{i}{2}\left(\wp(\xi) + \frac{a^2}{4\wp(\xi)^2 - {e_1}^2}\right)\, d\xi\,. \tag{6.53}$$

Making a similar substitution as above we get:

$$\sigma_2(\omega_3 + z) = \Re \int_{\omega_3}^{\omega_3+iz} \frac{i}{2}\left(\wp(-i\xi) + \frac{a^2}{4\wp(-i\xi)^2 - {e_1}^2}\right)(-i)d\xi \tag{6.54}$$

$$= \Re \int_{\omega_3}^{\omega_3+iz} -\frac{1}{2}\left(-\wp(\xi) + \frac{a^2}{4\wp(\xi)^2 - {e_1}^2}\right)\, d\xi \tag{6.55}$$

$$= \Re \int_{\omega_3}^{\omega_3+iz} \phi_1(\xi)\, d\xi \tag{6.56}$$

$$= \sigma_1(\rho(\omega_3 + z))\,. \tag{6.57}$$

And finally we can compute how the symmetry acts on σ_3 directly as we have an integrated expression already:

$$\sigma_3(\rho(\omega_3 + z)) = \frac{a}{8e_1}\ln\left|\frac{\wp(\rho(\omega_3+z)) - e_1}{\wp(\rho(\omega_3+z)) + e_1}\right| \tag{6.58}$$

$$= \frac{a}{8e_1}\ln\left|\frac{-\wp(\omega_3+z) - e_1}{-\wp(\omega_3+z) + e_1}\right| \tag{6.59}$$

$$= \frac{a}{8e_1}\ln\left|-\frac{\wp(\omega_3+z) + e_1}{\wp(\omega_3+z) - e_1}\right|^{-1} \tag{6.60}$$

$$= -\sigma_3(\omega_3 + z)\,. \tag{6.61}$$

Hence, the symmetry represented by ρ in the domain corresponds to a symmetry of the surface, namely the rigid motion:

$$R = \begin{pmatrix} 0 & -1 & 0 \\ 1 & 0 & 0 \\ 0 & 0 & -1 \end{pmatrix}, \tag{6.62}$$

which is a rotation of $\frac{\pi}{2}$ around the z-axis, followed by a reflection in (x, y) plane and so we have:

$$\vec{\sigma} \circ \rho = R\vec{\sigma}\,. \tag{6.63}$$

Now we want to look at how β affects the Costa surface:

$$\sigma_1(\omega_3 + z) = \Re \int_{\omega_3}^{\omega_3+z} \frac{1}{2}\left(\wp(\xi) - \frac{a^2}{4\wp(\xi)^2 - {e_1}^2}\right)\, d\xi\,. \tag{6.64}$$

Now we take the change of variables, $z \to \bar{\xi}$, hence $dz \to d\bar{\xi}$,. For our limits $\bar{\omega}_3 = \frac{1}{2} - \frac{i}{2} = \omega_3 - i$, so once again this is just a translation of our domain by one period and hence we can translate this back to our fundamental domain. We also know that $\wp(\bar{z}) = \overline{\wp(z)}$. So overall we get:

$$\sigma_1(\omega_3 + z) = \Re \int_{\omega_3}^{\omega_3+\bar{z}} \frac{1}{2}\left(\wp(\bar{\xi}) - \frac{a^2}{4\wp(\bar{\xi})^2 - {e_1}^2}\right)\, d\bar{\xi} \tag{6.65}$$

$$= \Re \int_{\omega_3}^{\omega_3+\bar{z}} \frac{1}{2}\left(\overline{\wp(\xi)} - \frac{a^2}{4\overline{\wp(\xi)}^2 - {e_1}^2}\right)\, d\bar{\xi}\,. \tag{6.66}$$

However since we are taking the real part of this integral, the bars of the integrand and the integration variable cancel, thus we get:

$$\sigma_1(\omega_3 + z) = \sigma_1(\beta(\omega_3 + z))\,. \tag{6.67}$$

For the second coordinate we see that:

$$\sigma_2(\omega_3 + z) = \Re \int_{\omega_3}^{\omega_3+z} \frac{i}{2}\left(\wp(\xi) + \frac{a^2}{4\wp(\xi)^2 - {e_1}^2}\right)\, d\xi\,. \tag{6.68}$$

After making our change of variables and substituting the identity for the Weierstrass function we arrive at:

$$\sigma_2(\omega_3 + z) = \Re \int_{\omega_3}^{\omega_3+\bar{z}} \frac{i}{2} \left(\overline{\wp(\xi)} + \frac{a^2}{4\overline{\wp(\xi)}^2 - e_1{}^2} \right) d\bar{\xi} \,. \tag{6.69}$$

Since we are taking the real part of i multiplied by the integrand, this is the same as taking the negative of the imaginary part, and since we have introduced a complex conjugate, the sign will have changed, hence:

$$\sigma_2(\omega_3 + z) = -\sigma_2(\beta(\omega_3 + z)) \,. \tag{6.70}$$

And once again, as we have an explicit formula for the third coordinate function, we can evaluate it directly:

$$\begin{aligned} \sigma_3(\beta(\omega_3 + z)) &= \frac{a}{8e_1} \ln \left| \frac{\wp(\beta(\omega_3 + z)) - e_1}{\wp(\beta(\omega_3 + z)) + e_1} \right| && (6.71) \\ &= \frac{a}{8e_1} \ln \left| \frac{\overline{\wp(\omega_3 + z)} - e_1}{\overline{\wp(\omega_3 + z)} + e_1} \right| && (6.72) \\ &= \sigma_3(\omega_3 + z) \,. && (6.73) \end{aligned}$$

We can now see that $\beta(\omega_3 + z)$ acts on our surface in $\mathbb{R}^3$ by reflecting in the (x, z) plane, which is given by the matrix:

$$B = \begin{pmatrix} 1 & 0 & 0 \\ 0 & -1 & 0 \\ 0 & 0 & 1 \end{pmatrix} \,, \tag{6.74}$$

and hence we see that:

$$\vec{\sigma} \circ \beta = B\vec{\sigma} \,. \tag{6.75}$$

We can visualise these symmetries by plotting a single fundamental unit of the Costa surface and where it maps under a given symmetry.

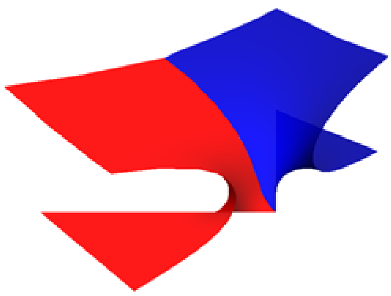

(a) A graphic showing a fundamental region of the Costa surface along with its symmetry under β.

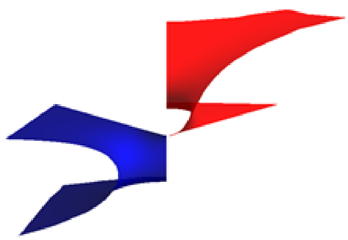

(b) A graphic showing a fundamental region of the Costa surface along with its symmetry under ρ.

Now we can show that the symmetry group of the Costa surface is indeed the dihedral group D_8 which has two generators, r and s, with the following relations, $r^4 = e$, $s^2 = e$, and $(sr)^2 = e$, where e is the identity element. Therefore, in total the group is $D_8 = \{e, r, r^2, r^3, s, sr, sr^2, sr^3\}$. We find that R and B, do indeed satisfy the relations $R^4 = \mathbb{I}$ and $B^2 = \mathbb{I}$, where $\mathbb{I}$ is the 3×3 identity matrix. So in total we have,

$$\mathbb{I} = \begin{pmatrix} 1 & 0 & 0 \\ 0 & 1 & 0 \\ 0 & 0 & 1 \end{pmatrix}, \qquad R = \begin{pmatrix} 0 & -1 & 0 \\ 1 & 0 & 0 \\ 0 & 0 & -1 \end{pmatrix}, \tag{6.76}$$

$$R^2 = \begin{pmatrix} -1 & 0 & 0 \\ 0 & -1 & 0 \\ 0 & 0 & 1 \end{pmatrix}, \qquad R = \begin{pmatrix} 0 & 1 & 0 \\ -1 & 0 & 0 \\ 0 & 0 & -1 \end{pmatrix}, \tag{6.77}$$

$$S = \begin{pmatrix} 1 & 0 & 0 \\ 0 & -1 & 0 \\ 0 & 0 & 1 \end{pmatrix}, \qquad SR = \begin{pmatrix} 0 & -1 & 0 \\ -1 & 0 & 0 \\ 0 & 0 & -1 \end{pmatrix}, \tag{6.78}$$

$$SR^2 = \begin{pmatrix} -1 & 0 & 0 \\ 0 & 1 & 0 \\ 0 & 0 & 1 \end{pmatrix}, \qquad SR = \begin{pmatrix} 0 & 1 & 0 \\ 1 & 0 & 0 \\ 0 & 0 & -1 \end{pmatrix}. \tag{6.79}$$

It is a simple calculation to verify that these matrices do indeed fulfil the algebraic relations of D_8. Each of these matrices maps the surface into itself, and hence this is the symmetry group of surface.

The fact that region III maps into the positive quadrant, as described in section 6.3.1 and that the symmetries of the Costa surface map these fundamental pieces into different quadrants of $\mathbb{R}^3$ is the first step Hoffman and Meeks use in their paper [11] to prove the Costa surface is embedded. They then go on to show that each of these fundamental units is embedded, and hence we can conclude that the entire surface is embedded.

Throughout this section we have been exploring the symmetries and properties of the Costa surface, by looking at small portions of it. We can put all of these regions together and view the surface in its entirety:

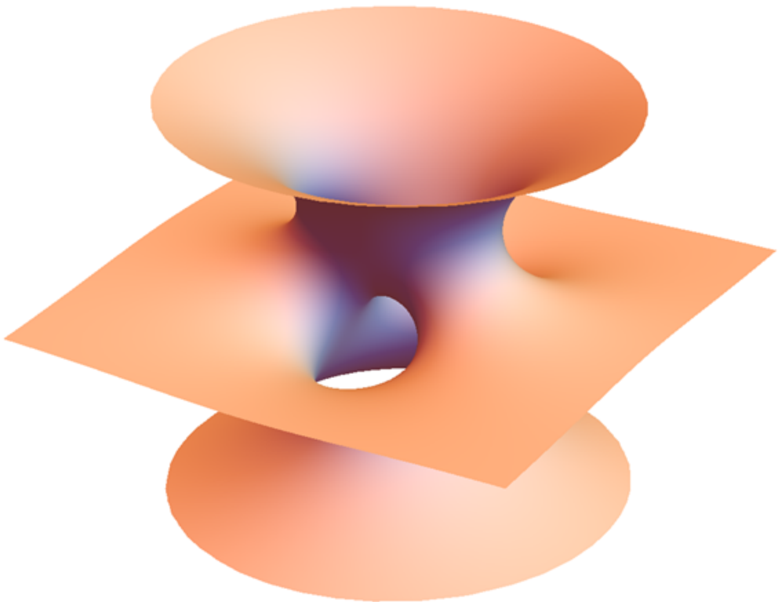

Figure 16: A plot of the Costa surface showing both catenoidal ends and the planar end.

6.4 Associate Family of the Costa Surface

Due to the fact it is not embedded, not much attention is paid to the associate family of the Costa surface, in fact after an extensive search it does not appear to have been covered in the literature. However there is definitely merit in looking at it as it provides an interesting case study of the features of associate families.

We shall start by considering changes to the planar end of the Costa surface. Looking at the associate family of the plane, parameterised by θ we see, by the fact that its Gauss map is constant, that the surface is in fact invariant with respect to θ. It is therefore obvious that the planar end of the Costa surface does not change i.e. it is still a planar end.

We also know that the catenoidal ends become helicoidal at $\theta = \frac{\pi}{2}$, and hence we do not expect the conjugate surface to be embedded, as we shall have two helicoids. These helicoids are indeed oriented in the opposite directions and offset by 90° from each other, however this is hard to see as *Wolfram Mathematica* was used to generate the images in figure 17 uses the principle log branch, and hence we can only see the section of the helicoid corresponding to angle between $-\pi$ and π. Developing techniques to visualise larger portions of the surface.

It is possible to graph the changes in the Costa surface computationally. Here we have used *Wolfram Mathematica* to produce the following plots of the associate family at various values of θ. The code for this can be found in Appendix B.

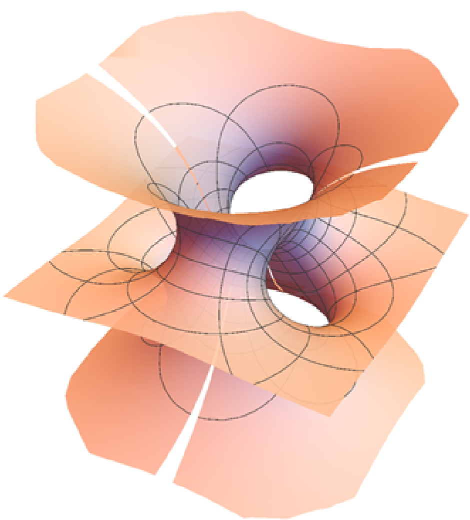

(a) $\theta = 0$

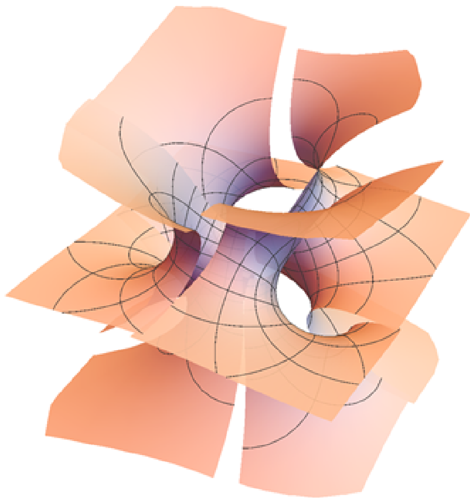

(b) $\theta = \frac{\pi}{10}$

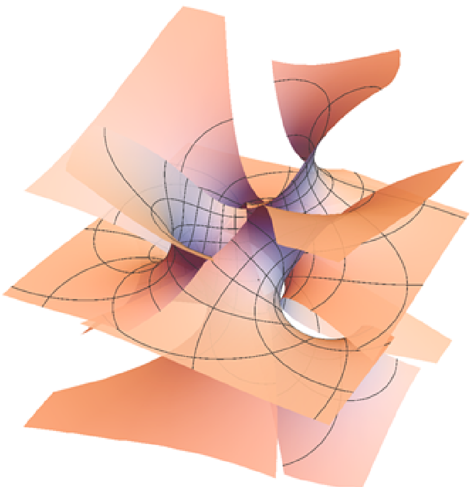

(c) $\theta = \frac{\pi}{5}$

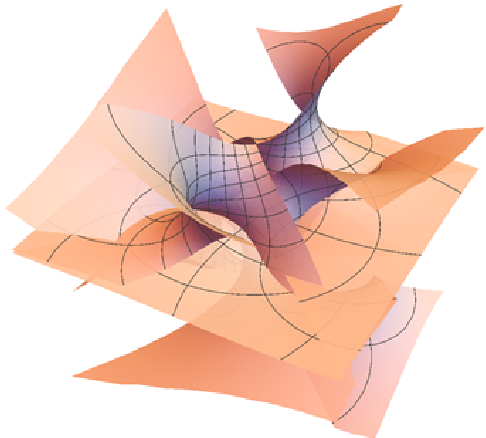

(d) $\theta = \frac{3\pi}{10}$

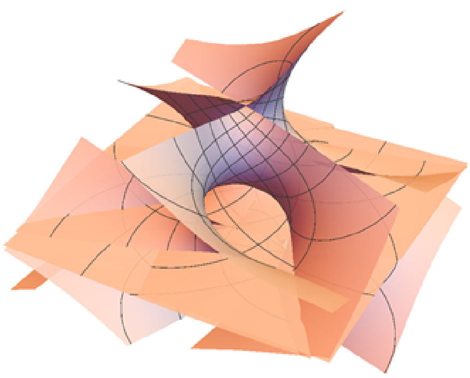

(e) $\theta = \frac{2\pi}{5}$

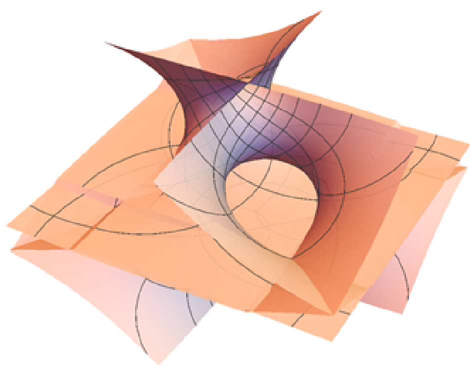

(f) $\theta = \frac{\pi}{2}$

Figure 17: Members of the associate family of the Costa surface, for values, $\theta \in \{0, \frac{\pi}{10}, \frac{\pi}{5}, \frac{3\pi}{10}, \frac{2\pi}{5}, \frac{\pi}{2}\}$.

7 Conclusion

In this paper we developed a formal theory of minimal surfaces using the basic geometric concepts of surfaces. We then unified the theory of minimal surfaces with complex analysis. From there we derived the Weierstrass representation which allowed us to study the properties of and plot the Enneper surface, the catenoid, and the helicoid. We discovered the Weierstrass representation is a powerful tool in the study of minimal surfaces as it allowed us to discover the underlying connection between two very different surfaces, the catenoid and helicoid, into a single family of surfaces.

We then defined the Weierstrass P function and examined its properties. We then used this in conjunction with the Weierstrass representation to prove the symmetries of the Costa surface directly from this symmetric function which a constituent of its representation.

Using the mathematical formalisms laid out in this paper, we were then able to study the associate family of the Costa surface, a topic rarely, if ever, discussed in the literature. We found that it is no longer embedded, but still highly structured and had interesting properties which would be an interesting topic of further study.

From here one could study generalisations of the Costa surface to higher genuses as laid out in [15]. It would be interesting to look at asymptotic behaviour of this family of surfaces.

Appendix A

Presented here are the calculations of the catenoid–helicoid associate family. We start with equation (5.44) and integrate each component. Firstly we can see that:

$$(\vec{\sigma}_\theta)_1(u_1,u_2) = \Re\left[e^{i\theta}\frac{1}{4}(e^{u_1+iu_2}+e^{-u_1-iu_2})\right] \tag{7.1}$$

$$= \frac{1}{4}\Re\left[(\cos(\theta)+i\sin(\theta))(e^{u_1}(\cos(u_2)+i\sin(u_2))+e^{-u_1}(\cos(u_2)-i\sin(u_2)))\right] \tag{7.2}$$

$$= \begin{matrix}\frac{1}{4}\Re[e^{u_1}(\cos(u_2)\cos(\theta)-\sin(u_2)\sin(\theta)+i\cos(\theta)\sin(u_2)+i\sin(\theta)\cos(u_2))+ \\ +e^{-u_1}(\cos(u_2)\cos(\theta)+\sin(u_2)\sin(\theta)-i\cos(\theta)\sin(u_2)+i\sin(\theta)\cos(u_2))]\end{matrix} \tag{7.3}$$

$$= \frac{1}{4}e^{u_1}(\cos(v)\cos(\theta)-\sin(u_2)\sin(\theta))+\frac{1}{4}e^{-u_1}(\cos(u_2)\cos(\theta)+\sin(u_2)\sin(\theta)) \tag{7.4}$$

$$= \frac{1}{2}\cosh(u_1)\cos(u_2)\cos(\theta)-\frac{1}{2}\sinh(u_1)\sin(u_2)\sin(\theta)\,. \tag{7.5}$$

Now for the second coordinate function:

$$(\vec{\sigma}_\theta)_1(u_1,u_2) = \Re\left[\frac{i}{4}(e^{u_1+iu_2}-e^{-u_1-iu_2})\right] \tag{7.6}$$

$$= \frac{1}{4}\Re\left[(-\sin(\theta)+i\cos(\theta))(e^{u_1}(\cos(u_2)+i\sin(u_2))-e^{-u_1}(\cos(u_2)-i\sin(u_2)))\right] \tag{7.7}$$

At this point we shall take the real part

$$(\vec{\sigma}_\theta)_1(u_1,u_2) = -\frac{1}{4}(\sin(\theta)e^{u_1}\cos(u_2)-\cos(\theta)e^{u_1}\sin(u_2)+\sin(\theta)e^{-u_1}\cos(u_2)-\cos(\theta)e^{-u_1}\sin(u_2)) \tag{7.8}$$

$$= \frac{1}{2}\sinh(u_1)\cos(u_2)\sin(\theta)-\frac{1}{2}\cosh(u_1)\sin(u_2)\cos(\theta)\,. \tag{7.9}$$

And finally we can see the last coordinate function is:

$$(\sigma_\theta)_3\frac{1}{2} = \Re\left[e^{i\theta}(u_1+iu_2)\right] \tag{7.10}$$

$$= \Re\left[(\cos(\theta)+i\sin(\theta))(u_1+iu_2)\right] \tag{7.11}$$

$$= u_1\cos(\theta)-u_2\sin(\theta) \tag{7.12}$$

So the surface map is given by:

$$\vec{\sigma}_\theta(u_1,u_2) = \begin{pmatrix} \frac{1}{2}\cosh(u_1)\cos(u_2)\cos(\theta)-\frac{1}{2}\sinh(u_1)\sin(u_2)\sin(\theta) \\ \frac{1}{2}\sinh(u_1)\cos(u_2)\sin(\theta)-\frac{1}{2}\cosh(u_1)\sin(u_2)\cos(\theta) \\ u_1\cos(\theta)-u_2\sin(\theta) \end{pmatrix} \tag{7.13}$$

Now let us preform a quick check for the values $\theta = 0$ and $\theta = \frac{\pi}{2}$ to ensure this does coincide with the catenoid and helicoid respectively:

$$\vec{\sigma}_0(u_1, u_2) = \begin{pmatrix} \frac{1}{2}\cosh(u_1)\cos(u_2)\cos(0) - \frac{1}{2}\sinh(u_1)\sin(u_2)\sin(0) \\ -\frac{1}{2}\cosh(u_1)\sin(u_2)\cos(0) + \frac{1}{2}\sinh(u_1)\cos(u_2)\sin(0) \\ u_1\cos(0) - u_2\sin(0) \end{pmatrix} \tag{7.14}$$

$$= \begin{pmatrix} \frac{1}{2}\cosh(u_1)\cos(u_2) \\ -\frac{1}{2}\cosh(u_1)\sin(u_2) \\ u_1 \end{pmatrix} \tag{7.15}$$

This does indeed give the catenoid, now to check for the helicoid:

$$\vec{\sigma}_{\frac{\pi}{2}}(u_1, u_2) = \begin{pmatrix} \frac{1}{2}\cosh(u_1)\cos(u_2)\cos(\frac{\pi}{2}) - \frac{1}{2}\sinh(u_1)\sin(u_2)\sin(\frac{\pi}{2}) \\ -\frac{1}{2}\cosh(u_1)\sin(u_2)\cos(\frac{\pi}{2}) + \frac{1}{2}\sinh(u_1)\cos(u_2)\sin(\frac{\pi}{2}) \\ u_1\cos(\frac{\pi}{2}) - u_2\sin(\frac{\pi}{2}) \end{pmatrix} \tag{7.16}$$

$$= \begin{pmatrix} -\frac{1}{2}\sinh(u_1)\sin(u_2) \\ \frac{1}{2}\sinh(u_1)\cos(u_2) \\ -u_2 \end{pmatrix} \tag{7.17}$$

which again is the expected result.

Appendix B

Shown below is the *Wolfram Mathematica* code which was used to create the plots of the associate family of the Costa surface in section 6.4.

```
inv = WeierstrassInvariants[{0.5, 0.5 I}]
e = WeierstrassP[0.5, inv]
a = 2 Sqrt[2 Pi] e

x[x_, y_, t_] = 0.5 Re[E^(I t) (-WeierstrassZeta[u + I v, inv]     + Pi (u + I v)
    + Pi/(2 e) (WeierstrassZeta[u + I v - 1/2, inv]
    - WeierstrassZeta[u + I v - I/2, inv])
    + (Pi^2/(4 e) - I (e Pi)/8))]

y[u_, v_, t_] = 0.5 Re[E^(I t) (-I WeierstrassZeta[u + I v, inv]
    - I Pi (u + I v)
    - Pi/(2 e) (I WeierstrassZeta[u + I v - 1/2, inv]
    - I WeierstrassZeta[u + I v - I/2, inv])
    + (Pi^2/(4 e) + I (e Pi)/8))]

z[x_, y_, t_] = Re[E^(I t) a/(8 e)
    Log[(WeierstrassP[x + I y, inv] - e) /
        (WeierstrassP[x + I y, inv] + e)]
    - (a Pi I)/(8 e)]

R = 3
L = {0, Pi/10, Pi/5, (3 Pi)/10, (2 Pi)/5, Pi/2}
plots = Table[
  ParametricPlot3D[{x[u, v, i], y[u, v, i], z[u, v, i]}, {u, 0,
    1}, {v, 0, 1}, PlotRange -> {{-R, R}, {-R, R}, {-R, R}},
   Boxed -> False, Axes -> False, PlotPoints -> 100,
   PlotStyle -> {Opacity[0.9], FaceForm[LightRed, LightRed]}], {i, L}]
```

References

[1] Meeks III, W; Pérez, J. *The classical theory of minimal surfaces.* Bulletin of the American Mathematical Society 48.3, 325-407 (2011)

[2] McNeil, I. *An Encyclopedia of the History of Technology.* (2002)

[3] Hildebrandt, S; Tromba A. *Mathematics and Optimal Form.* Scientific American Library (1985)

[4] Drukker, N; Gross, D; Ooguri, H. *Wilson Loops and Minimal Surfaces* (1999)

[5] Costa, C. *Examples of a Complete Minimal Immersion in* R^3 *of Genus One and Three Embedded Ends.* Bil. Soc. Bras. Mat. 15, 47-54 (1984)

[6] Neu, J. *Kinks and the minimal surface equation in Minkowski space.* Physica D: Nonlinear Phenomena Volume 43, Issues 2–3, 421-434. (1990)

[7] Rowland, T; Weisstein, E. *Poincaré's Lemma* MathWorld–A Wolfram Web Resource. http://mathworld.wolfram.com/PoincaresLemma.html

[8] Osserman, R. *A Survey of Minimal Surfaces.* (1986)

[9] Fang, Y. *Lectures on Minimal Surfaces in* $\mathbb{R}^3$*.* (1996)

[10] James, R. *Advanced Calculus.* Belmont, CA: Wadsworth. (1966)

[11] Hoffman, D; Meeks III, W. *A complete embedded minimal surface in* $\mathbb{R}^3$ *with genus one and three ends.* J. Differential Geom. 21 (1985)

[12] Hoffman, D. *Global theory of minimal surfaces*, American Mathematical Society, Providence, RI, for the Clay Mathematics Institute, Cambridge (2005)

[13] Bagemihl F. *Analytic Continuation and the Schwarz Reflection Principle.* Proceedings of the National Academy of Sciences of the United States of America. Pages 378-380. (1964)

[14] Carathéodory, C. *Thoery of Functions of a Complex Variable, Vol. 2.* §§343-346. (1954)

[15] Hauswirth, L; Pacard, F. *Higher genus Riemann minimal surfaces.* Invent. Math., 169(3) 569–620 (2007)